Establishment and validation of molecular predictive models for understanding survival and susceptibility of *Vibrio parahaemolyticus* in seafood stored at low temperature

by

Chao Liao

A thesis submitted to the Graduate Faculty of
Auburn University
in partial fulfillment of the
requirements for the Degree of
Master of Science

Auburn, Alabama
May 8, 2016

Keywords: *Vibrio parahaemolyticus*, Seafood, Molecular predictive model, PCR-DGGE, real-time RT-PCR, Cold adaptation

Approved by

Luxin Wang, Chair, Assistant Professor of Animal Sciences
Yifen Wang, Professor of Biosystem Engineering
Leonard N. Bell, Professor of Food Science

Abstract

Vibrio parahaemolyticus has been a leading cause of pathogenic diseases to human health after consumption of contaminated seafood. Microbial predictive models have been very important parts in quantitative microbiological risk assessment (QMRA) to help people control pathogens. However, it has been known that predictive models based on traditional methods (i.e. plate counting methods) are time-consuming and lab-intensive. Also, these methods are not able to count the microorganisms occurring in special states (e.g. viable but nonculturable state, VBNC, stressed state), leading to underestimated risk results.

In the first study, we simultaneously construct PCR-DGGE-based predictive models of *Listeria monocytogenes* and *Vibrio parahaemolyticus* on ready-to-eat shrimps when stored at 4^{o}C and 10^{o}C. A PCR-DGGE method was developed to enumerate *V. parahaemolyticus*. The Baranyi model was used to fit these data to molecular models (MMs). For *L. monocytogenes*, the MMs were growth models, which presented high goodness-of-fit as coefficients of determination (R^2) > 0.92 and bias factors (B_f) and accuracy factors (A_f) within the range of 1.0 to 1.1. In addition, compared with tradition models (TMs) based on plate counting methods, no significant difference (P > 0.05) was found when analyzing model parameters, lag phase (λ), or maximum growth rate (μ_{max}). However for *V. parahaemolyticus*, the molecular models (MMs) were inactivation models, which showed significant differences when compared with TMs. In summary, the DNA-based PCR-DGGE method is accurate and reliable when used to construct

growth models, but not suitable to establish inactivation models because DNA is also extracted from dead cells.

In the second study, in order to establish accurate and reliable inactivation MMs for *V. parahaemolyticus*, the RNA-based real-time RT-PCR was applied to develop MMs of *V. parahaemolyticus* in Eastern oysters (*Crassostrea virginica*) during storage at 0, 4, and 10^{o}C for 21 or 11 days. Also, we investigated the efficiency of an individual quick freezing (IQF) treatment on cold and non-cold adapted *V. parahaemolyticus*. MMs of *V. parahaemolyticus* were constructed based on real-time RT-PCR, and compared with TMs based on plate counting methods. The results were significantly different ($P < 0.05$) between the population reductions, inactivation rates, and the valid numbers of *V. parahaemolyticus*. Additionally, the result of IQF efficiency showed that cold adapted cells had a greater ability to resist adverse conditions resulting in less die-off. All indicate that MMs based on real-time RT-PCR are more specific, sensitive, and reliable to predict growth or inactivation of microorganisms.

Acknowledgments

I would like to express my sincere gratitude to my advisor, Dr. Luxin Wang; my committee members, Dr. Yifen Wang and Dr. Leonard N. Bell; our technician, Patty Tyler; every one of my friends, my lab mates, and classmates in Auburn. In addition, I would like to thank my advisor in Shanghai Ocean University (SHOU), Dr. Yong Zhao, and all of my lab mates and friends in SHOU. Additionally, I would like to thank my family.

Table of Contents

List of Tables

List of Illustrations

List of Abbreviations

V. parahaemolyticus	*Vibrio parahaemolyticus*
L. monocytogenes	*Listeria monocytogenes*
PCR-DGGE	Polymerase chain reaction-denaturing gradient gel electrophoresis
RT-PCR	Reverse transcription- Polymerase chain reaction
MMs	Molecular models
TMs	Traditional models
IQF	Individual quick freezing
TLH	Thermolabile hemolysin
TDH	Thermostable direct hemolysin
TRH	TDH-related hemolysin
T3SSs	Type III secretion systems
T6SSs	Type VI secretion systems
QMRA	Quantitative microbiological risk assessment
VBNC	Viable but non-culturable
R^2	Coefficients of determination
A	Maximal values
λ	Lag phase
μ_{max}	Maximum growth rates
B_f	Bias factor
A_f	Accuracy factor

ATCC	American Type Culture Collection
TSB	Tryptone soy broth
TCBS	Thiosulphate-citrate-bile salt sucrose
CFU	Colony Forming Units
OD	Phosphate-buffered-saline
FDA	Food and Drug Administration
FAO	Food and Agriculture Organization
PHP	Heat-cool pasteurization
HCP	Heat-cool pasteurization
HHP	High hydrostatic pressure
GRs	Growth rates
IRs	Inactivation rates
RMSE	Root mean square error

Chapter 1: Introduction

Seafood is part of a nutrient-rich and healthy diet, which has many benefits to human beings, including risk reduction of heart disease, neurologic development, and brain development (Iwamoto et al., 2010). The seafood category contains crustaceans (e.g. shrimp, lobster, and crab), mollusks (e.g. oysters, mussels, and clams), fish eggs (i.e. roe), and finfish (e.g. tuna and salmon) (Jahns et al., 2014). In recent decades, seafood consumption has increased worldwide, such as in China and the United States. In these countries, shrimp and oysters are some of the most popular seafood.

Litopenaeus vannamei is one of the largest cultured shrimp species, accounting for > 70% of worldwide farmed shrimp production. In 1988, *L. vannamei* was introduced into China. After several years of improved culturing skill, the yield of this shrimp has reached more than 60% of total seafood yields, and *L. vannamei* has become the most commonly consumed seafood in China (Huang et al., 2011).

In the United States, the oyster has been an iconic seafood product for a long time. Five kinds of oysters are cultured and consumed, Eastern oysters, Pacific oysters, Kumamoto oysters, Olympias oysters, and Belons oysters. The Gulf of Mexico coast has established a booming oyster industry, accounting for more than 86% of the commercial portion of oyster production in the United States with production bringing in nearly $75 million (Larsen et al., 2015).

Although seafood consumption provides many nutrients and is beneficial to human beings, it also comes with the potential risk of foodborne illness. Chemical, physical, and biological agents have been found in contaminated seafood. Compared with chemical and physical contaminations, foodborne illnesses caused by biological agents are more difficult to detect and can become widely occurring outbreaks. These biological agents include bacteria,

viruses, and parasites, which cause symptoms from mild gastroenteritis to life-threatening illness. Among these foodborne pathogens, *Vibrio parahaemolyticus* is the most commonly associated bacteria of reported infections related with seafood. It is a leading cause of gastroenteritis in the United States with an estimated 35,000 cases each year because of consuming contaminated seafood (Ye et al., 2013).

In recent years, in order control the risks of foodborne pathogens, quantitative microbiological risk assessment (QMRA) has been created as a tool to improve food safety and public health. QMRA of *V. parahaemolyticus* was carried out by the Food and Agricultural Organization (FAO) and World Health Organization (WHO) to estimate the risk of illness caused by consumption of contaminated seafood worldwide (FAO / WHO, 2011). QMRA consists of four parts: hazard identification, exposure assessment, hazard characterization, and risk characterization.

Predictive microbiology is a description of the responses of microorganisms to particular environmental conditions such as temperature, pH and water activity during the process of food production, transportation, and storage. Predictive models are based on mathematical functions to model the growth and survival of pathogenic microorganisms for the prediction of food safety and remaining shelf life of food products in the food chain (Baranyi and Roberts, 1995). In QMRA, predictive models provide numerous data to support an accurate and reliable exposure assessment that is an important section in QMRA.

The objective of this thesis is to establish predictive survival models of *V. parahaemolyticus* in two seafood matrices (Ready-to-eat shrimp and postharvest oysters) stored in cold temperatures (0, 4, and 10^{o}C). We utilized a traditional method (TCBS Plate counting method) and two molecular methods (PCR-DGGE and real-time RT-PCR) to collect survival

data of *V. parahaemolyticus* to construct traditional models (TMs) and molecular models (MMs). The two types of models (TMs and MMs) were compared to find which MMs provided the most reliable and accurate prediction of *V. parahaemolyticus* in seafood.

References

Baranyi J, Roberts TA. 1995. Mathematics of predictive food microbiology. Int. J. Food Microbiol. **26:** 199-218.

Huang YC, Yin ZX, Ai HS, Huang XD, Li SD, Weng SP, He JG. 2011. Characterization of WSSV resistance in selected families of *Litopenaeus vannamei*. Aquaculture **311:** 54-60.

Jahns L, Raatz SK, Johnson LK, Kranz S, Silverstein JT, Picklo MJ. 2014. Intake of seafood in the US varies by age, income, and education level but not by race-ethnicity. Nutrients **6:** 6060-6075.

Larsen AM, Rikard FS, Walton WC, Arias CR. 2015. Temperature effect on high salinity depuration of *Vibrio vulnificus* and *V. parahaemolyticus* from the Eastern oyster (*Crassostrea virginica*). Int. J. Food Microbiol. **192:** 66-71.

Food and Agriculture Organization of the United Nations / Word Health Organization. 2011. Risk assessment of *Vibrio parahaemolyticus* in seafood: interpretative summary and technical report. Microbiological Risk Assessment Series No 16. Rome: FAO.

Ye M, Huang Y, Gurtler JB, Niemira BA, Sites JE, Chen H. 2013. Effects of pre-or post-processing storage conditions on high-hydrostatic pressure inactivation of *Vibrio parahaemolyticus* and *V. vulnificus* in oysters. Int. J. Food Microbiol. **163:** 146-152.

Chapter 2

Literature Review

2.1 Characteristics of *Vibrio parahaemolyticus*

In recent years, the number of disease outbreaks caused by pathogens inhabiting coastal waters worldwide kept increasing. This has drawn a large amount of attention to food safety (Letchumanan et al, 2014). Among these pathogens, *Vibrio parahaemolyticus* (*V. parahaemolyticus*), a Gram-negative halophilic bacterium, exists in estuarine, marine, and coastal environments (Su and Liu, 2007; Zhang and Orth, 2013). Usually, *V. parahaemolyticus* is found in a free-swimming state due to the motility powered by a single polar flagellum (McCarter, 1999). Relying on environmental conditions, the classification of *V. parahaemolyticus* is based on a number of different somatic (O) and capsular (K) antigens (Nair et al., 2007).

This bacterium can be frequently isolated from various seafoods, including shrimp, oyster, codfish, sardine, flounder, clam, crab, and crawfish (Yan et al., 2014). Consumption of raw or under cooked seafood contaminated *V. parahaemolyticus* may cause acute gastroenteritis with symptoms including diarrhea, headache, vomiting, nausea, abdominal cramps, and a low fever. The infection can also cause septicemia that can be life threatening to individuals (Zhang and Orth, 2013).

V. parahaemolytcicus was first discovered in 1950 by Tsunesaburo Fujino during a large outbreak in Japan, which caused 272 illnesses (20 deaths) after consumption of shirasu (also called whitebait) (Fujino et al., 1953). Since then, *V. parahaemolyticus* has been found to account for 20% to 30% of food illnesses in Japan and many other Asian countries (Zhang et al., 2015). Additionally, it became the leading cause of gastroenteritis caused by the consumption of contaminated seafood in the United States and China (Newton et al., 2012; Wu et al., 2014).

2.2 Virulence factors of *Vibrio parahaemolyticus*

In past decades, outbreaks of *V. parahaemolyticus* diseases have increased around the world. Scientists have found several virulence factors in *V. parahaemolyticus* that cause these outbreaks, including thermostable direct hemolysin (TDH), tdh-related hemolysin (TRH), type III secretion systems (T3SS1 and T3SS2), and type VI secretion systems (T6SS1 and T6SS2) (Makino et al., 2003).

2.2.1 Thermostable direct hemolysin (TDH)

Although *V. parahaemolyticus* widely exists in marine and estuarine environments, most strains isolated are not pathogenic due to lack of the pathogenic genes *tdh* and/or *trh* (FDA, 2005; Gutierrez West et al., 2013). According to studies from Asia, Europe, and the U.S., approximately 0 to 6% of environmental samples contain *V. parahaemolyticus* with *tdh* or/and *trh* genes (Alam et al., 2002; Hervio-Heath et al., 2002). However, almost all of the *V. parahaemolyticus* isolated from clinically ill patients have the ability to produce TDH, which can lyse erythrocytes when plated on Wagatsuma agar. This process was named as the Kanagawa phenomenon (KP) (Miyamoto et al., 1969). *V. parahaemolyticus* strain with *tdh* gene also shows the Kanagawa phenomenon. Hence, TDH has been considered as the major virulence factor of *V. parahaemolyticus* (Hiyoshi et al., 2010). Nevertheless, studies have reported that about 1 to 2% of the environment samples are KP-positive and the rest are KP-negative (Alipour et al., 2014).

Researchers have found that TDH is an amyloid toxin, which can destroy the lipid micro-domains that resist cytotoxicity in the host cells (Ceccarelli et al., 2013). In addition, TDH can open a fairly large pore to allow water and ions to flow through the membrane of host cells,

which explains the mechanism behind the diarrhea caused by *V. parahaemolyticus* infection (Raghunath, 2014).

2.2.2 TDH-related hemolysin (TRH)

Epidemiological studies reported that some KP-negative clinical *V. parahaemolyticus* strains that do not encode the *tdh* gene may produce another hemolysin, named TRH, which is similar to TDH but which is heat labile (Ceccarelli et al., 2013). There is 67% homology between *trh* and *tdh* genes, but nucleotide variability on alleles of the *trh* gene is higher (Malcolm et al., 2015). Similar to TDH, the TRH can activate Cl^- channels to alter flux through membranes of host cells so as to cause diarrhea (Takahashi et al., 2000).

2.2.3 Type III secretion systems (T3SSs)

In 1996, a pandemic of *V. parahaemolyticus* O3:K6 strain, RIMD 2210633, was isolated from a patient having diarrhea symptoms in Japan (Hurley et al., 2006). Then, Makino et al. (2003) conducted genome sequencing for this strain and found that its genome was comprised of two circular chromosomes with 4832 genes. Meanwhile, a new type III system was identified on the chromosomes of this strain. Type III secretion systems are needle-like machinery, which inject bacterial protein effectors into membranes of host cells (Letchumanan et al., 2014). The T3SSs consist of 20 to 30 proteins stretching through the inner and outer bacterial membranes with a polymerized needle extending into extracellular space or the host cell membrane (Izore et al., 2011). Commonly, T3SS effectors can target the actin cytoskeleton, autophagy, and innate immune signaling. Pathogens can regulate systems up and down to meet their needs (Broberg et al., 2011).

2.2.3.1 T3SS1

The T3SS1 gene consists of 42 genes, which has 30 genes similar to T3SS from other microorganisms, such as *Yesinia spp.* and *Pseudomonas aeruginosa* (Makino et al., 2003). The T3SS1 system can be found in all environmental and clinical *V. parahaemolyticus* strains (Paranjpye et al., 2012). It can be regulated by releasing three interacting proteins (ExsC, ExsD, and ExsE) to control the activity of ExsA, a master transcriptional regulator. When it is under inducing conditions, the first step is the release of ExsE that leads to the secretion of ExsC. This will bind to ExsD to stimulate the release of ExsA, which then activates the transcription of T3SS1 (Zhou et al., 2010). There are three main effectors from the T3SS1 gene, VopQ (VP1680), VPA0450, and VopS (VP1686) that involve autophagy, membrane blebbing, cell rounding, and cell lysis. VopQ is produced to prevent the phagocytosis of the infecting bacteria (Sreelatha et al., 2013). VPA0450 can detach the plasma membrane from the actin cytoskeleton, leading to blebbing of the plasma membrane and lysis of the host cell (Zhang and Orth, 2013). The VopS targets and collapses the actin cytoskeleton so as to lead to cell rounding and shrinkage (Ceccarelli et al., 2013).

2.2.3.2 T3SS2

T3SS2 can only be found in clinical and pandemic *V. parahaemolyticus* strains. The gene is encoded on chromosome 2 (Paranjpye et al., 2012). T3SS2 is flanked by two *tdh* genes on a pathogenicity island (VPAI-7) (Zhang et al., 2012). In addition, T3SS2 has four major effectors, including VopC (VPA1312), VopT (VPA 1327), VopA/P (VPA1346), and VopL (VPA1370). The VopC (VPA1321) is an exotoxin that can prevent hydrolysis of GTP, which induces

alterations in the actin cytoskeleton to allow *V. parahaemolyticus* to enter into non-phagocytic host cells (Zhang et al., 2012). VopT (VPA1327) can change the small GTPase Ras to also prevent GTP hydrolysis that then facilitates *V. parahaemolyticus* infection. VopA/P may cooperate with VopT to block the activation of the MPK pathway (Broberg et al., 2011). The VopL (VPA1370) is a protein that can affect actin filament nucleation in host cells (Namgoong et al., 2011).

2.2.4 Type VI secretion systems (T6SSs)

The type VI systems, T6SS1 and T6SS2 are similar to the type III secretion systems, and are located on chromosomes 1 and 2 (Boyd et al., 2008). Studies have reported that the T6SS2 and the T3SS2 systems cooperate in the process of infection of a host. T6SS2 plays a role to assist *V. parahaemolyticus* in attaching to host cells, then T3SS2 releases effectors to cause cytotoxicity (Yu et al., 2012; Raghunath, 2014). Because the T6SS gene is present in all pandemic strains, it was also used as a virulence marker to discriminate pandemic and non-pandemic strains (Ceccarelli et al., 2013). Researchers found that T6SS1 is most active under warm marine-like conditions, and T6SS2 is active under low salt conditions. The quorum sensing and surface sensing of *V. parahaemolyticus* distinctly regulate these two systems (Salomon et al., 2013). Additionally, T6SS1 has a role in helping *V. parahaemolyticus* compete against other bacterial species, which can help *V. parahaemolyticus* increase its populations in marine systems during the summer months (Salomon et al., 2013).

2.3 Detection of *Vibrio parahaemolyticus*

With more research being done on *V. parahaemolyticus*, various selective media and other methods have been developed to qualitatively or quantitatively identify *V. parahaemolyticus*, such as thiosulphate citrate bile salts sucrose (TCBS), CHROMagar *Vibrio* (CV) agar, most probable number (MPN), and polymerase chain reaction (PCR).

2.3.1 Thiosulphate citrate bile salts sucrose (TCBS)

TCBS is the most widely used selective media for identification of *V. parahaemolyticus*. The components of TCBS contain ox bile (0.8%), NaCl (1%), and a condition of pH 8.6, which can inhibit other interfering microorganism growth. Because of the sucrose/bromothymol blue diagnostic system, *V. prahaemolyticus* colonies typically present themselves as round, opaque, green colonies 2 to 3 mm in diameter, while *V. cholerae* shows a yellow color and 2 to 3 mm in diameter colonies on TCBS agar (Bisha et al., 2012; Mrityunjoy et al., 2013). However, some studies proposed that TCBS was difficult to use to isolate and enumerate *V. parahaemolyticus* or *V. cholerae* in seafood samples because yellow or green colonies on TCBS could be produced by other sucrose-fermenting bacteria (Pinto et al., 2011).

2.3.2 CHROMagar *Vibrio*

CHROMagar *Vibrio* (CV) agar is a selective agar media containing colorimetric substrates for beta-galactosidase, which can differentiate ortho-nitrophenyl-beta-galactoside positive *V. parahaemolyticus* from other *Vibrio* species (Bisha et al., 2012). *V. parahaemolyticus* colonies develop as a mauve color on this medium. Some studies comparing CV with TCBS media revealed that CV was more accurate and specific to quantitatively detect *V. parahaemolyticus* in seafood samples (Duan and Su, 2005; Su and Liu, 2007).

2.3.3 Most probable number (MPN)

Most probable number (MPN) is a common bacterial enumerating method described by the US Food and Drug Administration Bacterial Analytical Manual (FDA, 1998). MPN is based on the probability of the numbers of positive growth bacteria in standard serially diluted samples (Sutton, 2010). The FDA has described the MPN method as using a 3-fold, 5-fold, or 10-fold serial dilution MPN tube with selective enrichment broth and selective agar medium for enumeration of *V. parahaemolyticus* in seafood samples (Kaysner and Depaola, 2004). However, MPN based on broth and media are time consuming and labor intensive, taking approximately 7-10 days (Tunung et al., 2011).

2.3.4 Polymerase chain reaction based techniques

In order to improve on the long wait time of MPN based broth and media, many studies combine the MPN method with the polymerase chain reaction (PCR) method to enumerate bacteria in seafood samples. This method then only takes 2 days (Martin et al., 2004). PCR and PCR-based techniques have been widely used in identification and enumeration of *V. parahaemolyticus* in food samples (Bej et al., 1999; Kaufman et al., 2004; Liao et al., 2015).

2.3.4.1 PCR

The PCR method applies designed DNA primers to target a fragment of a specific gene, and then detects the targeted bacteria through fragment amplification and electrophoresis. Researchers have developed the PCR method to detect pathogenic *V. parahaemolyticus* targeting *tdh* and *trh* genes, which encode thermostable direct hemolysin (TDH) and TDH-related

hemolysin (TRH) (Tada et al., 1992). *tlh* encoding is for a thermolabile hemolysin (TLH) and *toxR* genes are specific markers in *V. parahaemolyticus*. PCR targeting *tlh* and *toxR* genes are utilized to detect all of the *V. parahaemolyticus* in seafood samples (Bej et al., 1999; Kim et al., 1999).

2.3.4.2 Denaturing gradient gel electrophoresis

Polymerase chain reaction denaturing gradient gel electrophoresis (DGGE) is the most commonly used fingerprinting technique that has been applied to investigate microbial diversity of samples (Muyzer et al., 1993). In addition, Eiler and Bertilsson (2006) used PCR-DGGE to detect and quantify different *Vibrios* from environmental samples. Liao et al. (2015) simultaneously quantified *V. parahaemolyticus* and *Listeria monocytogenes*, and used quantitative data to construct predictive models.

2.3.4.3 Real-time PCR

With the advancement of PCR technology, real-time PCR has been developed as an accurate, specific, and sensitive method for quantitative detection of *V. parahaemolyticus* in seafood samples. Kaufman et al. (2004) reported real-time PCR targeting the *tlh* gene could be used for enumeration of total *V. parahaemolyticus* in oyster tissues. Takahashi et al. (2005) applied real-time PCR targeting the *toxR* gene of *V. parahaemolyticus* to quantify total *V. parahaemolyticus* populations in seawater and shellfish. Additionally, a multiplexed real-time PCR TaqMan assay was developed targeting four different genes to simultaneously detect different *V. parahaemolyticus*, such as *tlh* gene for total *V. parahaemolyticus*, *tdh* and *trh* genes

for pathogenic *V. parahaemolyticus*, and *ORF8* for pandemic *V. parahaemolyticus* O3:K6 (Ward and Bej, 2006).

References

Alam MJ, Tomochika KI, Miyoshi SI, Shinoda S. 2002. Environmental investigation of potentially pathogenic *Vibrio parahaemolyticus* in the Seto-Inland Sea, Japan. FEMS Microbiol. Lett. **208:** 83-87.

Alipour M, Issazadeh K, Soleimani J. 2014. Isolation and identification of *Vibrio parahaemolyticus* from seawater and sediment samples in the southern coast of the Caspian Sea. Comp. Clin. Path. **23:** 129-133.

Bej AK, Patterson DP, Brasher CW, Vickery MC, Jones DD, Kaysner CA. 1999. Detection of total and hemolysin-producing *Vibrio parahaemolyticus* in shellfish using multiplex PCR amplification of *tl*, *tdh* and *trh*. J. Microbiol. Methods **36:** 215-225.

Bisha B, Simonson J, Janes M, Bauman K, Goodridge LD. 2012. A review of the current status of cultural and rapid detection of *Vibrio parahaemolyticus*. Int. J. Food Sci. Tech. **47:** 885-899.

Boyd EF, Cohen AL, Naughton LM, Ussery DW, Binnewies TT, Stine OC, Parent MA. 2008. Molecular analysis of the emergence of pandemic *Vibrio parahaemolyticus*. BMC Microbiol. **8:** 110.

Broberg CA, Calder TJ, Orth K. 2011. *Vibrio parahaemolyticus* cell biology and pathogenicity determinants. Microbes Infect. **13:** 992-1001.

Ceccarelli D, Hasan NA, Huq A, Colwell RR. 2013. Distribution and dynamics of epidemic and pandemic *Vibrio parahaemolyticus* virulence factors. Front. Cell. Infect. Microbiol. **3:** 10-3389.

Di Pinto A, Terio V, Novello L, Tantillo G. 2011. Comparison between thiosulphate-citrate-bile salt sucrose (TCBS) agar and CHROMagar *Vibrio* for isolating *Vibrio parahaemolyticus*. Food Control **22:** 124-127.

Duan J, Su YC. 2005. Comparison of a Chromogenic Medium with Thiosulfate-Citrate-Bile Salts-Sucrose Agar for Detecting *Vibrio parahaemolyticus*. J. Food Sci. **70:** M125-M128.

Eiler A, Bertilsson S. 2006. Detection and quantification of *Vibrio* populations using denaturant gradient gel electrophoresis. J. Microbiol. Methods **67**

Fujino T, Okuno Y, Nakada D, Aoyama A, Fukai K, Mukai T, Ueho T. 1953. On the bacteriological examination of shirasu-food poisoning. Med. J. Osaka Univ. **4:** 299-304.

Hervio-Heath D, Colwell RR, Derrien A, Robert-Pillot A, Fournier JM, Pommepuy M. 2002. Occurrence of pathogenic *Vibrios* in coastal areas of France. J. Appl. Microbiol. **92:** 1123-1135.

Hiyoshi H, Kodama T, Iida T, Honda T. 2010. Contribution of *Vibrio parahaemolyticus* virulence factors to cytotoxicity, enterotoxicity, and lethality in mice. Infect. Immun. **78:** 1772-1780.

Hurley CC, Quirke A, Reen FJ, Boyd EF. 2006. Four genomic islands that mark post-1995 pandemic *Vibrio parahaemolyticus* isolates. BMC genomics **7:** 1.

Kaufman GE, Blackstone GM, Vickery MCL, Bej AK, Bowers J, Bowen MD, Epaola A. (2004). Real-time PCR quantification of *Vibrio parahaemolyticus* in oysters using an alternative matrix. J. Food Prot.**67:** 2424-2429.

Kaysner CA, DePaola A. 2004. *Vibrio*. Bacteriological Analytical Manual, Chapter 9. Arlington, VA : U.S. Food and Drug Administration.

Kim YB, Okuda J, Matsumoto C, Takahashi N, Hashimoto S, Nishibuchi M. 1999. Identification of *Vibrio parahaemolyticus* strains at the species level by PCR targeted to the toxR gene. J. Clin. Microbiol. **37:** 1173-1177.

Letchumanan V, Chan KG, Lee LH. 2014. *Vibrio parahaemolyticus*: a review on the pathogenesis, prevalence, and advance molecular identification techniques. Front. Microbiol. **5:** 10-3389.

Liao C, Peng ZY, Li JB, Cui XW, Zhang ZH, Malakar PK, Zhang WJ, Pan YJ, Zhao, Y. 2015. Simultaneous construction of PCR-DGGE-based predictive models of *Listeria monocytogenes* and *Vibrio parahaemolyticus* on cooked shrimps. Lett. Appl. Microbiol. 60(3), 210-216.

Izoré T, Job V, Dessen A. 2011. Biogenesis, regulation, and targeting of the type III secretion system. Structure **19:** 603-612.

Makino K, Oshima K, Kurokawa K, Yokoyama K, Uda T, Tagomori K, Kubota Y. 2003. Genome sequence of *Vibrio parahaemolyticus*: a pathogenic mechanism distinct from that of *V cholerae*. The Lancet **361:** 743-749.

Malcolm TTH, Cheah YK, Radzi CWJWM, Kasim FA, Kantilal HK, John TYH, Son R. 2015. Detection and quantification of pathogenic *Vibrio parahaemolyticus* in shellfish by using multiplex PCR and loop-mediated isothermal amplification assay. Food Control **47:** 664-671.

Martin B, Jofré A, Garriga M, Hugas M, Aymerich T. 2004. Quantification of *Listeria monocytogenes* in fermented sausages by MPN-PCR method. Lett. Appl. Microbiol. **39:** 290-295.

McCarter L. 1999. The multiple identities of *Vibrio parahaemolyticus*. J. Mol. Microbiol. Biotechnol. **1:** 51-57.

Miyamoto Y, Kato T, Obara Y, Akiyama S, Takizawa K, Yamai S. 1969. In vitro hemolytic characteristic of *Vibrio parahaemolyticus*: its close correlation with human pathogenicity. J. Bacteriol. **100:** 1147.

Mrityunjoy A, Eshita D, Kamal KD, Tasnia A, Muhammad AA, Rashed N. 2013. Microbiological study of sea fish samples collected from local markets in Dhaka city. Int. Food Res. J. **20**.

Muyzer G, De Waal EC, Uitterlinden AG. 1993. Profiling of complex microbial populations by denaturing gradient gel electrophoresis analysis of polymerase chain reaction-amplified genes coding for 16S rRNA. Appl. Environ. Microbiol. **59:** 695-700.

Nair GB, Ramamurthy T, Bhattacharya SK, Dutta B, Takeda Y, Sack DA. 2007. Global dissemination of *Vibrio parahaemolyticus* serotype O3: K6 and its serovariants. Clin. Microbiol. Rev. **20:** 39-48.

Newton A, Kendall M, Vugia DJ, Henao OL, Mahon BE. 2012. Increasing rates of Vibriosis in the United States, 1996–2010: review of surveillance data from 2 systems. Clin. Infect. Dis. **54:** S391-S395.

Namgoong S, Boczkowska M, Glista MJ, Winkelman JD, Rebowski G, Kovar DR, Dominguez R. 2011. Mechanism of actin filament nucleation by *Vibrio* VopL and implications for tandem W domain nucleation. Nat. Struct. Mol. Biol. **18:** 1060-1067.

Paranjpye R, Hamel OS, Stojanovski A, Liermann M. 2012. Genetic diversity of clinical and environmental *Vibrio parahaemolyticus* strains from the Pacific Northwest. Appl. Environ. Microbiol. **78:** 8631-8638.

Raghunath P. 2014. Roles of thermostable direct hemolysin (TDH) and TDH-related hemolysin (TRH) in *Vibrio parahaemolyticus*. Front. Microbiol. **5.**

Robin T, Ghazali FM, Mohd Adzahan N, Kumar Kantilal H, Nakaguchi Y, Nishibuchi M, Radu S. 2011. Rapid detection and enumeration of pathogenic *Vibrio parahaemolyticus* in raw vegetables from retail outlets. Int. Food Res. J. **18:** 67-78.

Salomon D, Gonzalez H, Updegraff BL, Orth K. 2013. *Vibrio parahaemolyticus* type VI secretion system 1 is activated in marine conditions to target bacteria, and is differentially regulated from system 2. PLoS One **8:** e61086.

Sreelatha A, Bennett TL, Zheng H, Jiang QX, Orth K, Starai VJ. 2013. *Vibrio* effector protein, VopQ, forms a lysosomal gated channel that disrupts host ion homeostasis and autophagic flux. Proc. Natl. Acad. Sci. **110:** 11559-11564.

Su YC, Liu C. 2007. *Vibrio parahaemolyticus*: a concern of seafood safety. Food Microbiol. **24:** 549-558.

Sutton S. 2010. The most probable number method and its uses in enumeration, qualification, and validation. J. Val. Technol. **16:** 35.

Tada J, Ohashi T, Nishimura N, Shirasaki Y, Ozaki H, Fukushima S, Takeda Y. 1992. Detection of the thermostable direct hemolysin gene (*tdh*) and the thermostable direct hemolysin-related hemolysin gene (*trh*) of *Vibrio parahaemolyticus* by polymerase chain reaction. Mol. Cell. Probes **6:** 477-487.

Takahashi A, Sato Y, Shiomi Y, Cantarelli VV, Iida T, Lee M, Honda T. 2000. Mechanisms of chloride secretion induced by *thermostable direct haemolysin* of *Vibrio parahaemolyticus* in human colonic tissue and a human intestinal epithelial cell line. J. Med. Microbiol. **49:** 801-810.

Takahashi H, Hara-Kudo Y, Miyasaka J, Kumagai S, Konuma H. 2005. Development of a quantitative real-time polymerase chain reaction targeted to the toxR for detection of *Vibrio vulnificus*. J. Microbiol. Methods **61:** 77-85.

US Food and Drug Administration (FDA). 1998. Bacteriological Analytical Manual Online. Available at 〈http://www.cfsan.fda.gov/~ebam/bam-toc.html〉, accessed July 13, 2006.

US Food and Drug Administration (FDA), 2005. Quantitative Risk Assessment on the Public Health Impact of Pathogenic *Vibrio parahaemolyticus* in Raw Oysters. Available at 〈 http://www.cfsan.fda.gov/~dms/vpra-toc.html〉, accessed June 22, 2006.

Ward LN, Bej AK. 2006. Detection of *Vibrio parahaemolyticus* in shellfish by use of multiplexed real-time PCR with TaqMan fluorescent probes. Appl. Environ. Microbiol. **72:** 2031-2042.

West CKG, Klein SL, Lovell CR. 2013. High frequency of virulence factor genes *tdh*, *trh*, and *tlh* in *Vibrio parahaemolyticus* strains isolated from a pristine estuary. Appl. Environ. Microbiol. **79:** 2247-2252.

Wu Y, Wen J, Ma Y, Ma X, Chen Y. 2014. Epidemiology of foodborne disease outbreaks caused by *Vibrio parahaemolyticus*, China, 2003–2008. Food Control **46:** 197-202.

Yan J, Liu Y, Wang Y, Xu X, Lu Y, Pan Y, Shi D. 2014. Effect of physiochemical property of Fe3O4 particle on magnetic lateral flow immunochromatographic assay. Sens. Actuators B. Chem. **197:** 129-136.

Yu Y, Yang H, Li J, Zhang P, Wu B, Zhu B, Fang W. 2012. Putative type VI secretion systems of *Vibrio parahaemolyticus* contribute to adhesion to cultured cell monolayers. Arch. Microbiol. **194:** 827-835.

Zhang H, Lu L, Liang J, Huang Q. 2015. Knowledge, attitude and practices of food safety amongst food handlers in the coastal resort of Guangdong, China. Food Control **47:** 457-461.

Zhang L, Krachler AM, Broberg CA, Li Y, Mirzaei H, Gilpin CJ, Orth K. 2012. Type III effector VopC mediates invasion for *Vibrio* species. Cell Rep. **1:** 453-460.

Zhang L, Orth K. 2013. Virulence determinants for *Vibrio parahaemolyticus* infection. Curr. Opin. Microbiol. **16:** 70-77.

Zhou X, Konkel ME, Call DR. 2010. Regulation of type III secretion system 1 gene expression in *Vibrio parahaemolyticus* is dependent on interactions between ExsA, ExsC, and ExsD. Virulence **1:** 260-272.

Chapter 3

First Paper

Simultaneous construction of PCR-DGGE-based predictive models of *Vibrio parahaemolyticus* and *Listeria monocytogenes* on cooked shrimps

Chao Liao[a], Zhiyun Peng[a], Jibing Li[a], Xiaowen Cui[a], Pradeep Kumar Malakar[a, d], Weijia Zhang[a,b,c], Yingjie Pan[a,b,c], Yong Zhao[a,b,c*]

[a]*College of Food Science and Technology, Shanghai Ocean University, No. 999 Hu Cheng Huan Road, Shanghai, 201306, China*

[b]*Laboratory of Quality & Safety Risk Assessment for Aquatic Products on Storage and Preservation (Shanghai), Ministry of Agriculture, No. 999 Hu Cheng Huan Road, Shanghai, 201306, China*

[c]*Shanghai Engineering Research Center of Aquatic-Product Processing & Preservation，No. 999 Hu Cheng Huan Road, Shanghai, 201306, China*

[d]*Institute of Food Research, Norwich Research Park, Colney, Norwich, NR4 7UA, United Kingdom*

* Corresponding author and reprint requests

Yong Zhao

College of Food Science and Technology

Shanghai Ocean University

(This paper has been accepted by Letter in Applied Microbiology)

Abstract

The aim of this study was to simultaneously construct PCR-DGGE-based predictive models of *Listeria monocytogenes* and *Vibrio parahaemolyticus* on cooked shrimps at 4 and 10°C. Calibration curves were established to correlate peak density of DGGE bands with microbial counts. Microbial counts derived from PCR-DGGE and plate methods were fitted by Baranyi model to obtain molecular models (MMs) and traditional models (TMs). For *L. monocytogenes*, growing at 4 and 10°C, MMs were constructed. It showed good evaluations of coefficients of determination ($R^2 > 0.92$), bias factors (B_f) and accuracy factors (A_f) ($1.0 \leq B_f \leq A_f \leq 1.1$). Moreover, no significant difference was found between MMs and TMs when analyzed on lag phase (λ), maximum growth rate (μ_{max}) and growth data ($P > 0.05$). But for *V. parahaemolyticus*, inactivated at 4 and 10°C, MMs show a significant difference ($P < 0.05$) when compared with TMs. Taken together, these results suggest that PCR-DGGE based on DNA can be used to construct growth models, but it is inappropriate for inactivation models yet. This is the first report of developing PCR-DGGE to simultaneously construct multiple MMs.

Significance and Impact of the Study

It has been known for a long time that microbial predictive models based on traditional plate methods are time-consuming and labor-intensive. Denaturing gradient gel electrophoresis (DGGE) has been widely used as a semi-quantitative method to describe a complex microbial community. In our study, we developed DGGE to quantify bacterial counts and simultaneously established two molecular models (MMs) to describe the growth and survival of two bacteria (*Listeria monocytogenes* and *Vibrio parahaemolyticus*) at 4 and 10°C. We demonstrated that PCR-DGGE could be used to construct growth models. This work provides a new approach to

construct MMs and thereby facilitates predictive microbiology and QMRA (Quantitative Microbial Risk Assessment).

Introduction

Listeria monocytogenes and *Vibrio parahaemolyticus* are common foodborne pathogens that are major causes of worldwide gastroenteritis and listeriosis (Zarei et al. 2012). To assess the pathogenic risk, a number of predictive models describing the growth of *L. monocytogenes* and *V. parahaemolyticus* have been investigated (Ohkochi et al. 2013; Parveen et al. 2013). Generally, predictive modelling is based on microbial growth data collected by plate methods. Nevertheless, the process is rather time-consuming and labor-intensive, and it takes at least 3–5 days to collect a group of data for constructing a predictive model (Wang et al. 2011). Where background microbial flora is present, the plate results are easily subject to be disturbed. Also, plate methods cannot detect the bacteria in the viable but non-culturable (VBNC) state (Oliver 2005). Recently, Ye et al. (2013) developed molecular models (MMs) based on real-time PCR to describe the growth of *L. monocytogenes* in vacuum-packaged chilled pork. However, real-time PCR still has some limitations (Bonetta et al. 2010), which can detect different target bacteria only by amplifying the different specific genes of different target bacteria, whereas polymerase chain reaction–denaturing gradient gel electrophoresis (PCR-DGGE) can simultaneously detect different bacteria by amplifying an universal DNA sequence, which has been widely recognized as a rapid microbial detection method (Ercolini 2004).

PCR-DGGE is considered as a semi-quantitative method. Some drawbacks lead to unreliable results due to biases in primer annealing, base pair mismatches and limitation in DGGE resolution (Petersen and Dahllöf, 2005). Nevertheless, a calibration curve is one approach

that can compensate for experimental variability during the experimental process, thereby reducing the inherent biases to the smallest amount possible.

In this study, we established calibration curves exhibiting the relationship between peak density data of DGGE bands and microbial counts. By referring to calibration curves and linear curves, peak density data can be transformed into microbial counts, thus bacteria can be quantified. Eventually, MMs based on PCR-DGGE were constructed to describe the growth of *L. monocytogenes* and *V. parahaemolyticus* on cooked shrimps at 4 and 10°C. It is expected that MMs based on PCR-DGGE would have a great applicability in food safety and quantitative microbiological risk assessment (QMRA).

Results and discussion

Bacterial counts obtained by traditional plate method

In this study, the traditional plate methods were used as a control to quantify two bacteria (*V. parahaemolyticus* and *L. monocytogenes*). At 4 and 10°C, *L. monocytogenes* grew but *V. parahaemolyticus* died on cooked shrimps. Rutherford et al. (2007) and Yoon et al. (2008) have reported that 4 and 10°C are suitable growth conditions for *L. monocytogenes* but unsuitable for *V. parahaemolyticus*.

Bacterial counts obtained by PCR-DGGE method

In DGGE fingerprint profiles, the amount and peak density of DGGE bands can indirectly reflect the diversity and quantity of microorganisms. We transformed the peak density into bacterial counts by calibration curves. In Fig. 3.1a, the DGGE profile shows the peak density of the upper bands (*L. monocytogenes*) increases in each lane, but that of the lower bands (*V.*

parahaemolyticus) decreases from the initial day to the 14th day at 4°C. The peak density of two bacteria bands increases from the initial day to the seventh day at 10°C (Fig. 3.1b).

This study was the first to develop the use of PCR-DGGE to quantify bacteria and construct MMs. In Fig. 3.2, the DGGE profile exhibits decreasing peak density from the left to right lanes corresponding to serial 10-fold dilutions of two bacterial suspensions. In Fig. 3.3, the mathematical function of calibration curve of *L. monocytogenes* is $y = -2762.76 + 568.2x$ and that of *V. parahaemolyticus* is $y = -2677.775 + 615.5x$. The peak density can be transformed into bacterial counts by the two functions.

Mathematical models fitting

The Baranyi model was used to fit data derived from PCR-DGGE and traditional plate methods. Fig. 3.4 shows molecular models (MMs) and traditional models (TMs) of *L. monocytogenes* and *V. parahaemolyticus* at 4 and 10°C fitted by the Baranyi model. For *L. monocytogenes*, all of the predictive models have increasing trends (Fig. 3.4a,b). For *V. parahaemolyticus*, all of the predictive models except for the molecular model at 10°C have decreasing trends. Junttila et al. (1988) have reported that the proper growth temperature of *L. monocytogenes* ranges from 1 to 45°C, and *V. parahaemolyticus* could die at temperatures below 12°C (Yang et al. 2012). Basically 4°C is a low enough temperature to cause *V. parahaemolyticus* to die. Thereafter, the DNA of the dead bacteria degrades continuously leading to the decline of the DGGE curve at 4°C (Fig. 3.4c). At 10°C, a small part of the population of *V. parahaemolyticus* is still growing but most die. Wang et al. (2014) also reported similar results. Thus, the growth rate is lower than death rate, leading to the decline of the plate counting curve while the DGGE curve at 10°C (Fig. 3.4d) is increasing because DNA can be extracted from

both viable and dead bacteria (Nogva et al. 2003). In this study, DNA degradation of dead bacteria is slower than the reproduction of new bacteria, thereby resulting in an increasing trend in MMs.

The large gaps that occurred between molecular and traditional models of *V. parahaemolyticus* at 4 and 10°C might be explained as follows. Firstly, part of the *V. parahaemolyticus* population entered the VBNC or stressed state (Slimani et al. 2012). Secondly, part of the overall DNA came from dead bacteria. Thirdly, some extracellular DNA may be extracted (Reichert-Schwillinsky et al. 2009). Therefore, molecular models are not appropriate for describing bacterial inactivation in this study, but it is worth further research to solve these problems.

Validation of MMs based on PCR-DGGE

All of the predictive models were fitted by the Baranyi function. The R^2, B_f and A_f were calculated to analyze the predictive feasibility of predictive models. Meanwhile, A, λ and μ_{max} were used to conduct a one-way ANOVA test to evaluate the difference between MMs and TMs (Ye et al. 2013).

For *L. monocytogenes* at 4 and 10°C, all of the R^2 (> 0.92) and B_f, A_f ($1.0 \leq B_f \leq A_f \leq 1.1$) (Table 3.1) suggest the MMs of *L. monocytogenes* have good predictive capability and feasibility. For comparison between MMs and TMs, both of them are growth models and stayed consistent (Fig. 3.4a,b). Moreover, except for A, no significant differences were found between λ and μ_{max} values of molecular and traditional models (Table 3.1). In addition, for whole growth data, no significant difference was calculated between the two predictive models. Before entering the stationary phase, no significant difference was found between the two models at 4°C (*P* =

0.514 > 0.05) and 10°C ($P = 0.177 > 0.05$). However, as curves entered the stationary phase, significant differences ($P < 0.05$) were found between the two models. It may be that the dead bacteria DNA did not degrade and along with the viable bacteria, increased the amount of DNA to lead to a higher predicted bacterial count by MMs than plate methods. This problem may be solved by using an RNA-based method or dead cell inhibitors (such as propidium monoazide, PMA) in further studies.

For *V. parahaemolyticus*, the R^2 of the molecular models are < 0.5 (Table 3.1), which suggests that the MMs of *V. parahaemolyticus* have a poor predictive capability. In Fig. 3.4c,d, almost all of the MMs and TMs are inactivation models except for MM at 10°C. Additionally, a large gap was observed between the two predictive models. The A, λ and μ_{max} values of molecular models show significant differences from traditional models (Table 3.1). Furthermore, a one-way ANOVA test on growth data reveals a highly significant difference ($P < 0.01$) between the two predictive models.

On the whole, PCR-DGGE based on DNA can be used in the construction of MMs of *L. monocytogenes* at 4 and 10°C, but it is not suited to *V. parahaemolyticus* at 4 and 10°C.

Materials and methods

Preparation of bacterial strains and food sample

Bacterial strains, *L. monocytogenes* ATCC 19115 and *V. parahaemolyticus* ATCC 33847, were obtained from the China Center of Industrial Culture Collection (Beijing, China).

The two bacterial strains were stored at −80°C in media with 25% glycerol. For activation of bacteria, 100-μl suspensions of *L. monocytogenes* were transferred to a tube containing nine ml tryptic soy broth (TSB), and *V. parahaemolyticus* were added into a TSB tube with 3% (w/w)

sodium chloride. The tubes were incubated at 37°C for 18 to 20 h. Then, 100-µl suspensions from the two tubes were, respectively, transferred to two new tubes with fresh TSB which were incubated at 37°C for 10 to 12 h (Wang et al. 2014). Afterwards, the two bacterial suspensions were detected at 600 nm (OD600), and several 10-fold dilutions were done to obtain a concentration of about 10^4 to 10^5 CFU ml^{-1}. The diluted bacterial suspensions were mixed 1:1 as the inoculum.

Shrimps were purchased from a local market in Shanghai and stored at −80°C until use. The selected shrimps (10 ± 1 g) were cooked to simulate home cooking with water for 10 min and then air dried in a biological safety cabinet for 10 min. Each boiled shrimp was inoculated on its abdomen with 100-µl of bacterial inoculum by pipette. Afterwards, the inoculated shrimps were packed in sterile stomacher bags (one shrimp per bag) (Interscience, Saint Norn, France) and stored at 4 and 10°C in duplicate.

Enumeration of *Listeria monocytogenes* and *Vibrio parahaemolyticus*

In total, fourteen experimental points were set for each temperature. The experimental intervals were one day at 4°C and a half day at 10°C, respectively. Each cooked shrimp was added to 90 ml of sterile 0.85% NaCl solution and homogenized for two min using a stomacher (Bag Mixer 400; Interscience) at room temperature.

Traditional plate method

For microbial enumeration, 100-µl of 10-fold serially diluted shrimp homogenates were spread on two selective plates (each plate in two replicates), PALCAM for *L. monocytogenes* and thiosulfate-citrate-bile salts-sucrose agar (TCBS) for *V. parahaemolyticus* (Beijing Land Bridge

Technology Company Ltd., Beijing, China). After incubation at 37°C for 24 h, *L. monocytogenes* and *V. parahaemolyticus* were counted (Zhang et al.2014).

Molecular method

DNA extraction from shrimp samples

Shrimp homogenates (1 ml) were aseptically transferred to a 1.5-ml sterile centrifuge tube and concentrated by centrifugation at 13,400 × *g* for 2 min. The pellets were stored at -80°C until used.

Bacterial DNA of *L. monocytogenes* and *V. parahaemolyticus* was extracted using the TIANamp Bacteria DNA Kit (Tiangen Biotech Co., Ltd., Beijing, China) according to the manufacturer's instruction with a modification involving prolonging the processing time of lysozyme to 0.5 h.

Calibration curve

To construct calibration curves correlating the peak density of DGGE bands with the bacterial counts, two pure cultures were incubated to reach an expected concentration (*L. monocytogenes*, 6.4×10^8 CFU ml^{-1}; *V. parahaemolyticus*, 2.8×10^8 CFU ml^{-1}), and then separately diluted for a serial dilution of 10-fold. The gradient concentrations of the two bacteria were from 10^8 to 10^4 CFU ml^{-1}. Subsequently, DNA was extracted from 1ml suspensions of each serially diluted bacteria. Then, the DNA of the two bacteria were used in the PCR-DGGE experiment. Last, the gradient concentrations of the two bacteria and the corresponding peak density data from the DGGE bands were utilized to establish calibration curves. The DGGE

fingerprinting profiles were analyzed by Quantity One software 4. 6. 2 (Bio Rad, USA). Peak density values of each bands in profiles were obtained.

PCR-DGGE assay

Primer V3-2 (5′-ATTACCGCGGCTGCTGG-3′) and Primer V3-3 (5′CGCCCGCCGCGCGCGGCGGGCGGGGCGGGGGCACGGGGGGCCTACGGGAGGCAG CAG 3′) were used to amplify V3 region of the 16S rDNA (Muyzer et al. 1993).

PCR amplification was performed with 20-µl reaction system containing 10-µl of Premix Ex Taq (Takara, Japan), 8-µl of ddH_2O, 0.5 µl of each primer and 1 µl of DNA template. The PCR program was conducted as follows: initial denaturation at 95°C for 3 min; 25 cycles of denaturation at 95°C for 1 min; annealing at 55°C for 1 min and extension at 72°C for 30 s; final extension at 72°C for 5 min and stored at 10°C (Xie et al. 2012).

DGGE analysis was carried out with DCode Universal Mutation Detection System (Bio-Rad, Berkeley, California, USA). Electrophoresis was performed in poly acrylamide gels [8% (w/v) acrylamide/bis-acrylamide ratio of 37.5 : 1] containing a 40 to 60% urea–formamide denaturing gradient [100% corresponds to 7 mol/l urea and 40% (v/v) formamide]. The denaturing gels were polymerized for 1 h. Then, a 5-ml non-denaturing stacking gel was injected on top of the denaturing gel, and a 16-well comb was inserted into the non-denaturing gel. After 1 h of gel solidification, 15 µl of PCR samples was loaded into each well and the gels were subjected to a constant voltage of 60 V for 16 h at 60°C in 1× TAE Buffer. After electrophoresis, the DGGE gels were stained with SYBR green (1 µl of SYBR green in 10 ml of ddH_2O) for 30 min and photographed under UV light (Xie et al. 2012).

Predictive models of *Listeria monocytogenes* and *Vibrio parahaemolyticus* on cooked shrimp

TMs were based on data derived from traditional plate methods, and MMs were based on the data obtained from PCR-DGGE. The Baranyi model was chosen as it provided a good fit to the growth data with meaningful microbiological parameters. The Baranyi model function is shown as follows (Baranyi et al. 1993):

$$y(t) = y_0 + \mu_{max}A(t) - \frac{1}{m}\ln\left(1 + \frac{e^{m\mu_{max}A(t)} - 1}{e^{m(y_{max} - y_0)}}\right)$$

$$A(t) = t + \frac{1}{\nu}\ln\left(\frac{e^{-\nu t} + q_0}{1 + q_0}\right) \quad (1)$$

In this equation, y: the logarithm of bacteria count at any given time, $\log_{10}$ CFU ml^{-1}; y_0 and y_{max} are the initial values and the maximum values of y; A: the asymptote is the maximal value reached; μ_{max}: the maximum value of relative growth rate; λ: lag phase; m, ν, q_0: model coefficients.

Evaluation of predictive models

To evaluate the goodness of fit of models, R^2, B_f and A_f were calculated. The bias factor (B_f) measures the relative average deviation of the predicted and observed bacterial growth. The accuracy factor (A_f) indicates the spread of the results around the predicted values. In this study, $1.0 \leq B_f \leq A_f \leq 1.1$ was defined as a satisfactory limit (Yang et al. 2012; Ye et al. 2013). So as to validate molecular models, A, λ and μ_{max} were compared with traditional models by one-way ANOVA test from SPSS statistics 17.0 software (SPSS, Chicago, USA). It is a technique used to compare the difference of two or more samples (Tabachnick and Fidell 2012). Evaluation parameter functions are shown as follows (Ye et al. 2013):

$$R^2 = 1 - \frac{\sum_{i=1}^{n}(predicted - observed)^2}{\sum_{i=1}^{n}(observed - mean)^2} \quad (2)$$

$$Bias\ factor = 10^{\left(\frac{\sum \log(predicted/observed)}{n}\right)} \quad (3)$$

$$Accuracy\ factor = 10^{\left(\frac{\sum |\log(predicted/observed)|}{n}\right)} \quad (4)$$

In these equations, n stands for the number of observations; predicted, observed and mean stand for the predicted values, observed values and average values, respectively.

Acknowledgements

This research was supported by the National Natural Science Foundation of China (31271870), the project of Science and Technology Commission of Shanghai Municipality (14DZ1205100, 14320502100, 12391901300), Key Project of Shanghai Agriculture Prosperity through Science and Technology (Grant: 2014, 3-5), Cross-Discipline Project (B5201120040).

References

Baranyi J, Roberts T, McClure P. 1993. A non-autonomous differential equation to model bacterial growth. Food Microbiol. **10:** 43–59.

Bonetta S, Bonetta S, Ferretti E, Balocco F, Carraro E. 2010. Evaluation of Legionella pneumophila contamination in Italian hotel water systems by quantitative real-time PCR and culture methods. J. Appl. Microbiol. **108:** 1576–1583.

Ercolini D. 2004. PCR-DGGE fingerprinting: novel strategies for detection of microbes in food. J. Microbiol. Methods **56:** 297–314.

Junttila JR, Niemelä S, Hirn J. 1988. Minimum growth temperatures of *Listeria monocytogenes* and non-haemolytic *listeria*. J. Appl. Microbiol. **65:** 321–327.

Muyzer G, De Waal EC, Uitterlinden AG. 1993. Profiling of complex microbial populations by denaturing gradient gel electrophoresis analysis of polymerase chain reaction-amplified genes coding for 16S rRNA. Appl. Environ. Microbiol. **59:** 695–700.

Nogva HK, Dromtorp S, Nissen H, Rudi K. 2003. Ethidium monoazide for DNA-based differentiation of viable and dead bacteria by 5′-nuclease PCR. Biotechniques **34:** 804–813.

Ohkochi M, Koseki S, Kunou M, Sugiura K, Tsubone H. 2013 Growth Modeling of Listeria monocytogenes in Pasteurized Liquid Egg. J. Food Prot. **76:** 1549–1556.

Oliver JD. 2005. The viable but nonculturable state in bacteria. J. Microbiol. **43:** 93–100.

Parveen S, DaSilva L, DePaola A, Bowers J, White C, Munasinghe KA, Brohawn K, Mudoh M. 2013. Development and validation of a predictive model for the growth of *Vibrio parahaemolyticus* in post-harvest shellstock oysters. Int. J. Food Microbiol. **161:** 1–6.

Petersen DG, Dahllöf I. 2005. Improvements for comparative analysis of changes in diversity of microbial communities using internal standards in PCR-DGGE. FEMS Microbiol. Ecol. **53:** 339–348.

Reichert-Schwillinsky F, Pin C, Dzieciol M, Wagner M, Hein I. 2009 Stress-and growth rate-related differences between plate count and real-time PCR data during growth of *Listeria monocytogenes*. Appl. Environ. Microbiol. **75:** 2132–2138.

Rutherford TJ, Marshall DL, Andrews LS, Coggins PC, Wes Schilling M, Gerard P. 2007. Combined effect of packaging atmosphere and storage temperature on growth of *Listeria monocytogenes* on ready-to-eat shrimp. Food Microbiol. **24:** 703–710.

Slimani S, Robyns A, Jarraud S, Molmeret M, Dusserre E, Mazure C, Facon JP, Lina G. 2012. Evaluation of propidium monoazide (PMA) treatment directly on membrane filter for the enumeration of viable but non cultivable Legionella by qPCR. J. Microbiol. Methods **88:** 319–321.

Tabachnick BG, Fidell L. 2012. Using Multivariate Statistics: International Edition, Pearson.

Wang H, Cheng H, Wei D, Wang F. 2011. Comparison of methods for measuring viable E. coli cells during cultivation: great differences in the early and late exponential growth phases. J. Microbiol. Methods **84:** 140–143.

Wang JJ, Sun WS, Jin MT, Liu HQ, Zhang W, Sun XH, Pan YJ, Zhao Y. 2014. Fate of *Vibrio parahaemolyticus* on shrimp after acidic electrolyzed water treatment. Int. J. Food Microbiol. **179:** 50–56.

Xie J, Sun XH, Pan YJ, Zhao Y. 2012. Physicochemical properties and bactericidal activities of acidic electrolyzed water used or stored at different temperatures on shrimp. Food Res. Int. **47:** 331–336.

Yang C, Li Y, Zhou Y, Zheng W, Tian Y, Zheng T. 2012 Bacterial community dynamics during a bloom caused by *Akashiwo sanguinea* in the Xiamen Sea Area, China. Harmful Algae **20:** 132–141.

Yang ZQ, Jiao XA, Li P, Pan ZM, Huang JL, Gu RX, Fang WM, Chao GX. 2009 Predictive model of *Vibrio parahaemolyticus* growth and survival on salmon meat as a function of temperature. Food Microbiol. **26:** 606–614.

Ye K, Wang H, Zhang X, Jiang Y, Xu X, Zhou G. 2013. Development and validation of a molecular predictive model to describe the growth of *Listeria monocytogenes* in vacuum-packaged chilled pork. Food Control **32:** 246–254.

Yoon K, Min K, Jung Y, Kwon K, Lee J, Oh S. 2008. A model of the effect of temperature on the growth of pathogenic and nonpathogenic *Vibrio parahaemolyticus* isolated from oysters in Korea. Food Microbiol. **25:** 635–641.

Zarei M, Maktabi S, Ghorbanpour M. 2012. Prevalence of *Listeria monocytogenes, Vibrio parahaemolyticus, Staphylococcus aureus*, and *Salmonella spp.* in seafood products using multiplex polymerase chain reaction. Foodborne Pathog. Dis. **9:** 108–112.

Zhang Z, Xiao L, Lou Y, Jin M, Liao C, Malakar PK, Pan YJ, Zhao Y. 2014. Development of a multiplex real-time PCR method for simultaneous detection of *Vibrio parahaemolyticus, Listeria monocytogenes* and *Salmonella spp.* in raw shrimp. Food Control **51:** 31–36.

Table 3.1 Growth parameters of molecular and traditional models fitted by the Baranyi model for *Listeria monocytogenes* and *Vibrio parahaemolyticus* at 4 and 10°C

		L. monocytogenes		*V. parahaemolyticus*	
T		Molecular model	Traditional model	Molecular model	Traditional model
4°C	R^2	0.92	0.98	0.47	0.80
	A (log10 CFU ml-1	10.29 ± 0.07[a]	8.95 ± 0.05[b]	6.56 ± 0.10[a]	4.35 ± 0.07[b]
	λ (day)	1.65 ± 0.06[a]	1.79 ± 0.04[a]	6.84 ± 0.56[a]	1.29 ± 0.12[b]
	μ_{max} (CFU ml^{-1} day^{-1})	0.42 ± 0.04[a]	0.40 ± 0.03[a]	-0.21 ± 0.08[a]	-0.21 ± 0.02[a]
	B_f	1.002	1.000	1.003	1.001
	A_f	1.041	1.017	1.064	1.028
10°C	R^2	0.96	0.97	0.23	0.96
	A (log10 CFU ml-1	10.52 ± 0.09[a]	9.51 ± 0.03[b]	7.21 ± 0.09[a]	4.47 ± 0.02[b]
	λ (day)	1.01 ± 0.05[a]	1.07 ± 0.03[a]	0[a]	0.41 ± 0.06[b]
	μ_{max} (CFU ml^{-1} day^{-1})	1.49 ± 0.11[a]	1.31 ± 0.08[a]	0.33 ± 0.07[a]	-0.82 ± 0.03[b]
	B_f	1.000	1.000	1.004	1.000
	A_f	1.025	1.028	1.068	1.041

[a-b] different superscript letters show significant differences between the same growth parameter of traditional and molecular predictive models.

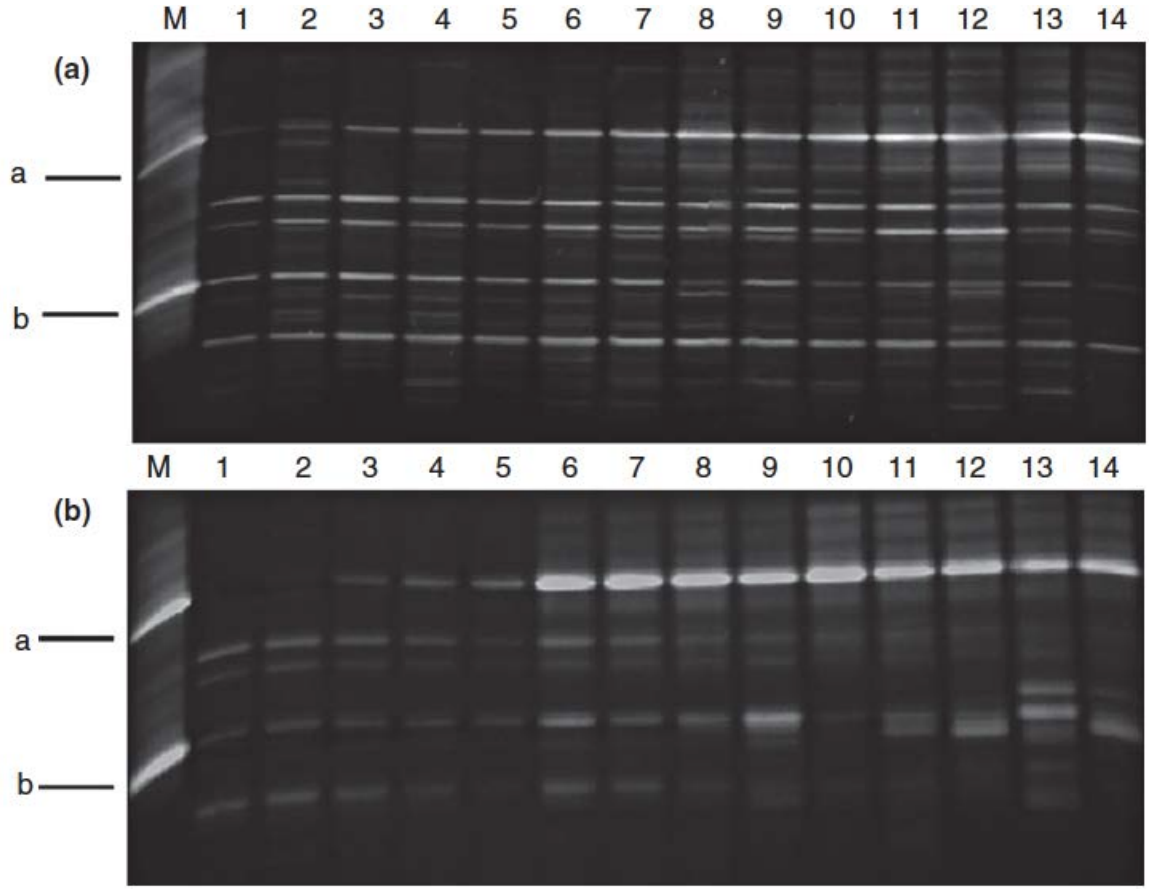

Figure 3. 1. (a) DGGE profile of samples at 4°C from the 1st to 14th day. (b) DGGE profile of samples at 10°C from the 0 to 7th day. Bands: a, *Listeria monocytogenes*; b, *Vibrio parahaemolyticus*. Lanes: M, markers; 1–14, 1st to 14th day at 4°C (1 day interval), 0 to 7th day at 10°C (0.5 day interval).

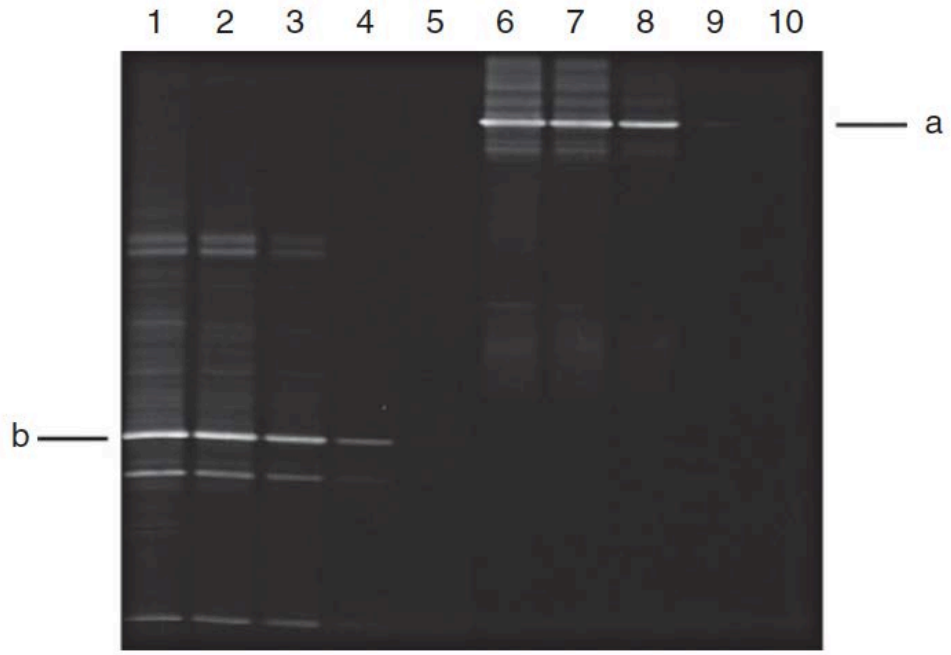

Figure 3. 2. DGGE profile of 10-fold diluted *Listeria monocytogenes* and *Vibrio parahaemolyticus*. Bands: a, *L. monocytogenes*; b, *V. parahaemolyticus*. Lanes: 1–5, bacterial concentrations of 10-fold dilutions from 8.45 to 4.45 log10 CFU ml-1; Lanes 6–10, bacterial concentrations of 10-fold dilutions from 8.8 to 4.8 log10 CFU ml-1.

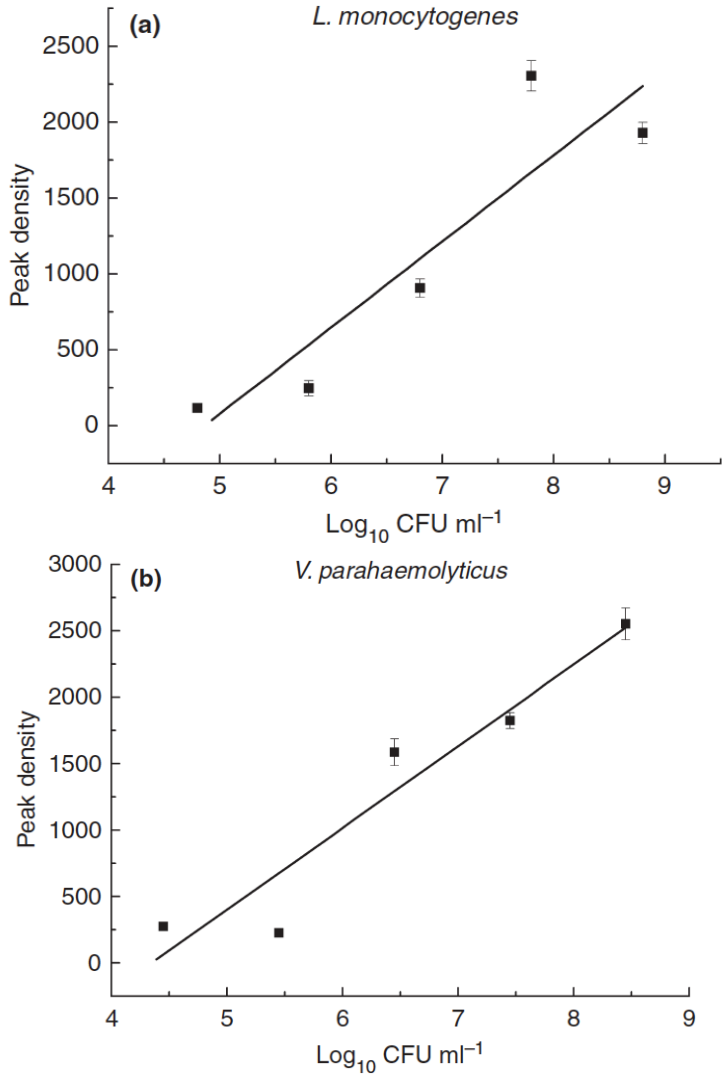

Figure 3. 3. Calibration curves of *L. monocytogenes* and *V. parahaemolyticus* based on peak density and corresponding ten-fold diluted bacterial counts. Black square: a, *L. monocytogenes*; b, *V. parahaemolyticus*. (a, b): (—) Linear fit. Error bars: Standard deviation of peak density.

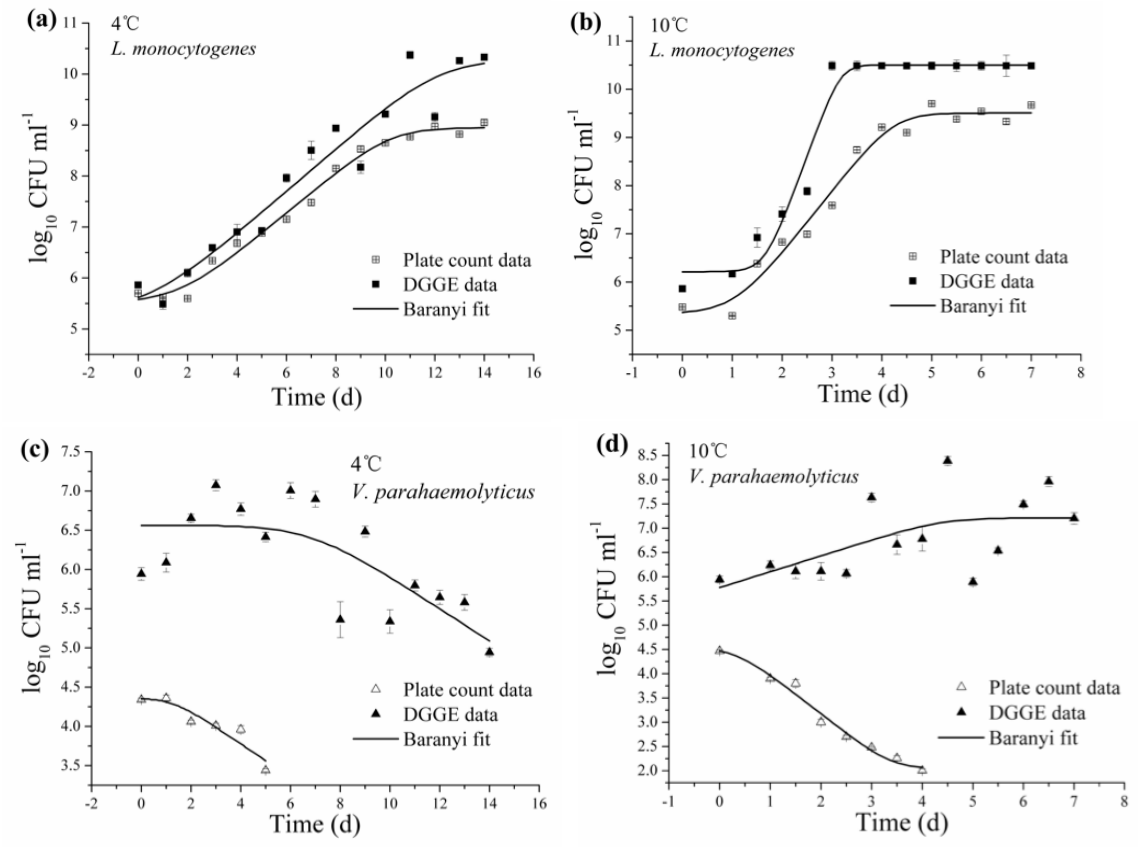

Figure 3. 4. (a, b) The molecular and traditional predictive models of *Listeria monocytogenes* at 4 and 10°C based on the Baranyi model. (c, d) The molecular and traditional predictive models of *Vibrio parahaemolyticus* at 4 and 10°C based on the Baranyi model. (a, b): (⊞) Plate count data; (■) DGGE data; (—) Baranyi fit; (c, d): (△) Plate count data; (▲) DGGE data; (—) Baranyi fit. Error bars: standard deviation of bacterial counts.

Chapter 4

Second Paper

Establishment and validation of RNA-based predictive models for understanding survival and susceptibility of low-temperature adapted *Vibrio parahaemolyticus* in oysters

Chao Liao [a], Yong Zhao [b], Luxin Wang [a,*]

[a] *Food Microbiology and Safety Lab, Department of Animal Sciences, Auburn University, Auburn, Alabama 36849, USA*

[b] *Laboratory of Quality & Safety Risk Assessment for Aquatic Products on Storage and Preservation (Shanghai), Ministry of Agriculture, Shanghai Ocean University, No. 999 Hu Cheng Huan Road, Shanghai, 201306, China*

*Corresponding author

Telephone: (334) 844-8146

E-mail: lzw0022@auburn.edu (L. Wang)

(This paper has been submitted to Applied and Environmental Microbiology)

Abstract

This study developed RNA-based predictive models describing the survival of *Vibrio parahaemolyticus* in Eastern oysters (*Crassostrea virginica*) during storage at 0, 4, and 10^{o}C, and investigated the efficiency of individual quick freezing (IQF) treatment on cold and non-cold adapted *V. parahaemolyticus*. Post-harvested oysters were inoculated with a cocktail of five *V. parahaemolyticus* strains and were then stored at 0, 4, and 10^{o}C for 21 or 11 days. A real-time RT-PCR assay targeting the *tlh* gene was used to evaluate the number of surviving *V. parahaemolyticus*, which was then used to establish primary molecular models (MMs). The MMs were compared with traditional models (TMs) based on data collected using the plate counting method. Based on MMs, *V. parahaemolyticus* decreased by 0.493, 0.362, and 0.238 $\log_{10}$ CFU/g at the end of storage, while the reductions of *V. parahaemolyticus* in TMs were 2.109, 1.579, and 0.894 $\log_{10}$ CFU/g for storage at 0, 4, and 10^{o}C. The inactivation rates (IRs) of MMs were -0.134, -0.0887, and -0.0732 $\log_{10}$ CFU/day for storage at 0, 4, and 10 °C, which were greater than those of TMs (-0.245, -0.152, and -0.121 $\log_{10}$ CFU/d). Higher valid *V. parahaemolyticus* numbers were predicted by using MMs. The efficiency of IQF was evaluated on cold-adapted *V. parahaemolyticus.* Results showed that non-cold adapted *V. parahaemolyticus* had a significantly higher die-off rate with the IQF treatment compared to cold adapted cells. RNA-based predictive MMs are more accurate and reliable models and can prevent false negative results compared to TMs. Cold-adaptation had a negative impact on the *V. parahaemolyticus* reduction efficiency of IQF.

Key words: *Vibrio parahaemolyticus*, Molecular predictive model, RNA, real-time RT-PCR, Cold adaptation

Introduction

Vibrio parahaemolyticus is a Gram-negative, halophilic asporogenous, and curved bacteria. It is a human pathogen that grows naturally in marine environments and can be isolated from various seafood, including oysters, fishes, and shrimps (Su and Liu, 2007). Oysters are a nutrient-rich seafood popular worldwide. In the United States, oyster consumption has increased in recent decades. Compared with consuming 10 to 12 pounds of seafood during the 1980s, the average American now eats approximately 16.5 pounds every year (Iwamoto et al., 2010). Unlike most other foods, oysters are often consumed raw or uncooked (Ye et al., 2012). Oysters feed by filtering large volumes of seawater. During this process, pathogenic microorganisms can accumulate and concentrate up to 100 times greater than those present naturally in seawater (Iwamoto et al., 2010; Fernandez-Piquer et al., 2011). The consumption of raw oysters has the potential to cause *V. parahaemolyticus* infection, with symptoms like watery diarrhea, abdominal cramps, nausea, vomiting, and even septicemia (Yang et al., 2009; DaSilva et al., 2012). The largest raw oyster associated outbreak happened in the United States in 1998 and caused 416 illnesses in 13 states (Iwamoto et al., 2010). In 2006, an outbreak of *V. parahaemolyticus* caused 177 illnesses in three states in the U.S. due to the consumption of raw oysters (Yoon et al., 2008). In the U.S., most cases (about 72.8%) of *Vibrio* infection occurred during summer months when water temperatures were warmer (Iwamoto et al., 2010). Other research also showed that higher densities of *V. parahaemolyticus* in harvested oysters were found in spring and summer months (Yoon et al., 2008; Parveen et al., 2013; Sobrinho et al., 2014).

All *V. parahaemolyticus* isolates contain the thermolabile hemolysin (*tlh*) gene, a marker gene that has been used to qualitatively or quantitatively detect *V. parahaemolyticus* in different food systems (Su and Liu, 2007). However, clinical illnesses caused by *V. parahaemolyticus*

strains are more closely associated with the expression of the thermostable direct hemolysin (*tdh*) and *tdh*-related hemolysin (*trh*) genes. The prevalence of *tdh* gene-positive isolates ranges from 3% to 70% and the prevalence of the *trh* gene ranges from 17 to 60% in all *V. parahaemolyticus* isolates (Fernandez-Piquer et al., 2011; Elexson et al., 2013).

One reason that *V. parahaemolyticus* has been a common problem in seafood is due to its ability to survive and persist over a range of temperatures. It was reported that the population of *V. parahaemolyticus* in oysters increased significantly when the temperature increased from 15^{o}C to 30^{o}C and decreased when temperatures were lower than 10^{o}C (Fernandez-Piquer et al., 2011; Parveen et al., 2013). To better ensure oyster safety and to control the levels of *V. parahaemolyticus* in harvested oysters, the National Shellfish Sanitation Program (NSSP) Guide requires that harvested shellfish should be cooled to below 10^{o}C (50^{o}F) within 12, 18, 24, and 36 h after harvesting when the average monthly maximum air temperature is ≥ 27^{o}C (80^{o}F), from 15 to 27^{o}C (60 to 80^{o}F), from 10 to 15^{o}C (50 to 60^{o}F), and below 10^{o}C (50^{o}F) respectively (FDA, 2013). To reduce *V. parahaemolyticus* levels in oysters, innovative post-harvest processing (PHP) technologies have been developed and approved by FDA (FDA, 2013). These include individual quick freezing (IQF), heat-cool pasteurization (HCP), and high hydrostatic pressure (HHP) (Meujo et al., 2010). These technologies have been commercially used by the seafood industry, thereby increasing the safety of raw oyster consumption. IQF is usually applied to half shell oysters and has served as an excellent way to preserve the moisture of oysters, thus keeping the products' freshness and quality. This method can also extend the oyster shelf life to well over one year (Cheney, 2010).

An important method used to validate post-harvest techniques and to monitor the behavior of *V. parahaemolyticus* is to establish predictive models. These models not only help

with validation and monitoring but can also contribute information in a risk assessment. Through mathematical functions, primary predictive models are developed to describe population dynamics of pathogenic and spoilage bacteria under different environmental conditions (Fernandez-Piquer et al., 2011). Based on the primary models, secondary predictive models are constructed to evaluate the effect of temperature on growth rates (GRs) or inactivation rates (IRs) of bacteria (Parveen et al., 2013). Predictive models have been developed to describe the behavior of *V. parahaemolyticus* in inoculated oyster (*Crassostrea gigas*) slurries over a range of temperatures from 10 to 30^{o}C, in inoculated Pacific oysters (*C. gigas*) at temperatures from 4 to 30^{o}C, as well as the behavior of naturally occurring *V. parahaemolyticus* in Eastern oysters (*Crassostrea virginica*) at temperatures ranging from 5 to 30^{o}C (Yoon et al., 2008; Fernandez-Piquer et al., 2011; Parveen et al., 2013).

Unfortunately, most of the current predictive models are constructed using plate counting methods. These methods are time-consuming, labor-intensive, and do not culture the bacteria in a viable but non-culturable (VBNC) or stressed state (Liao et al., 2015, Zhang et al., 2015). VBNC pathogenic bacteria are considered a threat to public health and food safety because they continue to retain their viability and ability to express their virulence (Ramamurthy et al., 2014). Therefore, predictive traditional models (TMs) based on plate counting methods may underestimate the populations of bacteria (Su et al., 2013; Ramamurthy et al., 2014). With the development of molecular quantitative methods, predictive models based on real-time PCR and PCR-DGGE methods have been reported to describe the survival and growth of *Listeria monocytogenes* and *V. parahaemolyticus* in food matrixes (Ye et al., 2013; Liao et al., 2015). However, all of these molecular methods are based on DNA, which can be extracted from both live and dead bacteria (Rudi et al., 2005; Wagner et al., 2008; Liao et al., 2015). Because RNA

can be extracted only from live bacteria, RNA based molecular methods serve as a more accurate method to quantitatively measure surviving *V. parahaemolyticus* cells (Tse, 2015).

The objectives of this study were to 1, establish and validate RNA-based predictive molecular models (MMs) using real-time RT-PCR to describe the survival of a *V. parahaemolyticus* cocktail in oysters at cold storage temperatures and 2, test the potential usage of real-time RT-PCR for validation of PHP by using the IQF treatment as an example.

Materials and Methods

1. Oysters

One-year-old Eastern oysters (*C. virginica*) were harvested from Mobile Bay, AL, USA, depurated under a flow-through depuration system for 7 days, and shipped overnight to the Food Microbiology lab by the Auburn University Marine Extension and Research Center (AUMERC) located at Dauphin Island, AL, USA. Upon arrival at the laboratory, oysters were washed to remove excess mud following protocols described by the American Public Health Association for the bacteriological examination of shellfish (Hunt et al., 1984). Oysters were then stored at 4^{o}C before inoculation.

2. Bacterial strains

A total of five *V. parahaemolyticus* strains (Table 1) were used in this study. Three strains were purchased from American Type Culture Collection (ATCC) *(*Manassas, VA, USA*)* and the other two strains were isolated from previous oyster studies. A liquid *V. parahaemolyticus* cocktail was prepared by growing individual strains in 10 ml of tryptone soy broth (TSB) *(*BBL/Difco Laboratories, Sparks, MD, USA) supplemented with 3% NaCl at 37°C for 18 h. The overnight fresh cultures were washed by centrifugation at 12,000 × *g* (Eppendorf, Hauppauge, NY, USA) for 3 min and re-suspended in 10 ml of phosphate-buffered-saline (PBS, pH 7.4). The optical density at 600 nm ($OD_{600\ nm}$) of each washed culture was adjusted to 1.7 ± 0.1. To mix the cocktail, equal volumes of each washed culture were taken and mixed in a 15 ml Falcon® sterile tube (VWR, Atlanta, GA, USA). The concentration of the *V. parahaemolyticus* cocktail was 1.12 × 10^{8} CFU/ml.

3. Oyster inoculation and storage

To inoculate the oysters, a 5 mm notch was drilled into the shell of each oyster approximately 50 mm from the hinge. After that, 100 µl of inoculum cocktail was injected into the muscle of the oyster using a sterile 1 ml syringe with a 23-gauge needle (Terumo, Somerset, NJ, USA) following the protocol described in previous reports (Garnier et al., 2007; Fernandez-Piquer et al., 2011). The inoculated oysters were kept flat on the bench top for 5 min to allow the liquid cultures to be absorbed by the oyster muscle before being stored at different temperatures.

Three storage temperatures and formats were chosen, 1, on ice (~0^{o}C); 2, in a 4^{o}C refrigerator; and 3, in a 10^{o}C refrigerator. For the 0^{o}C and 4^{o}C storage conditions, three sub-samples (three oysters/sample) of inoculated oysters were removed and analyzed once every day for the first week and then once every two days for two more weeks. For the 10^{o}C storage condition, oysters were removed and analyzed every 12 hours for the first week and then on days 9 and 11.

4. *V. parahaemolyticus* enumeration using plate count method

Thiosulphate-citrate-bile salt sucrose (TCBS) plates (BD, Sparks, MD, USA) were used to plate and enumerate the surviving *V. parahaemolyticus*. At each sampling point, three sets of three oysters were taken from each storage condition. The oysters were shucked and the meat was removed from the shell. Approximately 25 g of oyster meat from each storage condition were then placed in a filtered Whirl-pak® bag (Nasco, Fort Atkinson, WI, USA) with 225 ml of PBS. The mixture was homogenized by a Smasher™ lab blender (AES Chemunex, bioMérieux, France) at the normal speed for 2 min. The homogenized samples were diluted and plated. Colonies were enumerated after the plates were incubated at 37°C for 18 hours. In addition, 1 ml of every homogenized sample was removed, transferred into a 15 ml Falcon® sterile tube

(VWR, Atlanta, GA, USA), and stored at -80°C with 2 ml of RNA protect reagent (Qiagen, Hilden, Germany) for RNA extraction.

5. RNA extraction

In order to quantify the number of *V. parahaemolyticus* containing *tlh*, *tdh*, and *trh* genes using real-time RT-PCR, standard curves for the three target genes were established first. To extract the RNA for establishing the *tlh* gene-based standard curve, a serial of 10-fold dilutions of the *Vibrio* cocktail (with concentrations from 5.5×10^7 to 5.5×10^1 CFU/ml) were prepared. To extract the RNA for establishing the *tdh* gene-based standard curve, *V. parahaemolyticus* ATCC 43996 which contains *tdh* virulence gene and its serial dilution (with concentrations from 7.6×10^7 to 7.6×10^1 CFU/ml) was used. *V. parahaemolyticus* ATCC 17082 (the *trh* positive strain) was used to construct the *trh* gene standard curve. Similarly, a serial of 10-fold dilutions (6×10^7 to 6.0×10^1 CFU/ml) was used. RNA was extracted from 1 ml of each dilution solution using an RNeasy Mini Kit (Qiangen, CITY, CA, USA) following the manufacturer's manual.

To extract RNA from inoculated oyster samples, 1 ml of each stored homogenized sample solution (from step 4) was used. The same RNeasy Mini Kit was used to extract the RNA and all of the RNA samples were stored at -80°C immediately until analyzed.

The concentration and purity of all RNA samples was analyzed using a NanoVue Plus spectrophotometer (GE, Healthcare, Piscataway, NJ, USA). The cDNA was generated by reverse transcription from 10 µl of RNA from each sample by using the High Capacity cDNA Reverse Transcription kit (Applied Biosystem, Foster City, CA, USA) and then used for real-time PCR.

6. Real-time PCR

SYBR® Green real-time PCR was carried out on an ABI 7500 (Applied Biosystem, Foster City, CA, USA). Each reaction system consisted of 10 µl of solution from qSCript™ One-Step

qRT- PCR kit (Quanta Biosciences, Gaithersburg, MD, USA), 0.5 µl each of forward and reverse primers, 6 µl of RNase-free water, and 3 µl of cDNA templates. Standard curves were built by constructing regression lines with the X-axis being C*t* values and Y-axis being $\log_{10}$ CFU/ml. The standard curves were used to quantitatively calculate the surviving *V. parahaemolyticus* cells in inoculated oyster samples.

7. Primary model and secondary model

Data obtained from the plate counting method and real-time RT-PCR method were transformed to a $\log_{10}$ format. The means and standard deviations were calculated. For the survival model, the Baranyi equation (Baranyi et al., 1993) was chosen to fit the data, which was conducted in the DMfit section of Combase website (available at http://www.ifr.ac.uk/safety/dmfit/). The fitted model based on the plate counting method was defined as the traditional model (TM) and the model based on the real-time RT-PCR method was defined as the molecular model (MM). Parameters of models coefficient of determination (R^2), lag time (LT), inactivation rate (IR), initial value (IV), and final value (FV), were obtained. The Baranyi equation is as follows:

$$y(t) = y_0 + \mu_{max}A(t) - \frac{1}{m}\ln\left(1 + \frac{e^{m\mu_{max}A(t)} - 1}{e^{m(y_{max} - y_0)}}\right)$$

$$A(t) = t + \frac{1}{\nu}\ln\left(\frac{e^{-\nu t} + q_0}{1 + q_0}\right) \quad (1)$$

In this equation, y is the logarithm of the bacteria count at any given time, log cfu/ml; y_0 and y_{max} are the initial values and the maximum values of y; A: the asymptote is the maximal value reached; μ_{max}: the maximum value of relative growth or inactivation rate; m, ν, q_0: model coefficients.

The Arrhenius equation (Arrhenius, 1915) was applied for the establishment of the secondary model to describe the IR of *V. parahaemolyticus* in oysters as a function of temperature. The equation is as follows:

$$\ln r = \ln A - E_a/R(273.15+T) \quad (2)$$

Where r is the rate constant, T is the absolute temperature, E_a is the activation energy, R is the universal gas constant, and A is the collision factor. The equation was input into OriginPro 8.0 software (Origin Lab Corporation, Northampton, MA, USA), which was then used to fit the IR data to obtain a plot of ln r against T and the values of ln A and E_a/R.

8. Evaluation and validation of models

In order to evaluate the goodness-of-fit of the TMs and MMs, the root mean square error (RMSE), R^2, bias factor (B_f), and accuracy factor (A_f) were calculated. In addition, the inactivation parameters (LT, IR, IV, and FV) and analysis of variance (ANOVA) were calculated to assist in evaluating the performance of models. The TMs were compared with MMs through R^2, LT, IR, IV and FV values. To validate the MMs, a secondary validation model was built upon by conducting a replication experiment with a new batch of harvested Eastern oysters using the same inoculation and storage processes. For the validation of TMs, the fitted secondary TM of *V. parahaemolyticus* was compared with previously published models by Fernandez-Piquer et al. (2011). The estimated IRs of secondary models and validation models were analyzed by ANOVA. $P < 0.05$ was regarded as statistically different between groups of data.

9. Impact of cold-adaption of *V. parahaemolyticus* on IQF treatment

Because the RNA-based method can detect all viable cells, the last part of the research tested the efficacy of real-time RT-PCR to monitor the inactivation of *V. parahaemolyticus* treated with the quick freezing technique. To do this, inoculated oysters (procedures described

above) were stored at 0°C, 4°C, and 10°C for 5 days. On day 5, the oysters were taken out, shucked, and placed individually on a conveyer and frozen in a tunnel for individual quick freezing (IQF) (liquid CO_2 at -60°C for 10 min) and then stored at -20°C for 5 days before sampling. The number of surviving *V. parahaemolyticus* presenting in treated oysters was enumerated by both traditional plating methods and the real-time RT-PCR method. The control experiments were conducted for inoculated oysters with *V. parahaemolyticus* of similar concentration with oysters at day 5 for 0, 4, and 10°C.

Results

1. Primary models of *V. parahaemolyticus* in oysters

The final *V. parahaemolyticus* inoculation level in oysters was 5.45 ± 0.22 $\log_{10}$ CFU/g. By using the plate counting method and real-time RT-PCR, the populations of surviving *V. parahaemolyticus* in oysters were enumerated and calculated at different time intervals. For real-time RT-PCR, to convert the *Ct* values to cell counts, standard curves based on *tlh* and *tdh* genes were constructed (Fig. 4.1). The R^2 values were 0.999 and 0.998, and the equations were y = -3.849 x + 43.701 and y = -3.521 x + 42.139 for the *tlh* and *tdh* genes, respectively. Two groups of data, obtained from the plate counting method and the real-time RT-PCR method, were then fitted by Baranyi function (equation 1) to obtain primary TMs and MMs (Fig. 4.2).

The parameters of primary traditional and molecular models are listed in Table 2. For primary TMs, the average R^2 value for plate counting data fitted by Baranyi function (equation 1) of three storage temperatures (average of 0.943, 0.931 and 0.902) was 0.925. For storage at 0, 4, and 10°C, the initial values (IVs) of *V. parahaemolyticus* were 5.601, 5.293, and 5.463 $\log_{10}$ CFU/g and the final values (FVs) were 3.492, 3.714, and 4.569 $\log_{10}$ CFU/g. The inactivation

rates (IRs) showed an increasing trend with -0.245, -0.152, and -0.121 $\log_{10}$ CFU/day as the temperature increased from 0 to 4 and 10°C. The Lag times (LTs) were 1.931 and 1.605 days for 0 and 4°C, while it was zero for 10°C. It took 13.861, 13.219, and 10.123 days for *V. parahaemolyticus* to decrease from IVs to FVs for storage at 0, 4, and 10°C.

For primary MMs (Table 4.2), the average R^2 value for molecular data fitted by Baranyi function (equation 1) of the three storage temperatures was 0.859. The IVs were 5.428, 5.114, and 5.261 $\log_{10}$ CFU/g, and the FVs were 4.935, 4.752, and 5.023 $\log_{10}$ CFU/g for the 0, 4, and 10°C storage. The IRs also showed an increasing trend as temperature increased, -0.134, -0.0887, and -0.0732 $\log_{10}$ CFU/d for 0, 4, and 10°C storage. All of the LTs of molecular models of *V. parahaemolyticus* at 0, 4, and 10°C were zero. The times taken for *V. parahaemolyticus* to decrease from IVs to FVs were 5.881, 4.237, and 4.425 days for storage at 0, 4, and 10°C.

2. The survival of *V. parahaemolyticus* with *tdh* virulence gene during cold storage

The activity of *V. parahaemolyticus* containing the *tdh* virulence gene in oysters was monitored by real-time RT-PCR during cold storage at 0, 4, and 10°C (Fig. 4.3). The initial populations of these *V. parahaemolyticus* were 4.876, 4.704, and 4.924 $\log_{10}$ CFU/g and the final populations were 4.663, 4.297, and 4.687 $\log_{10}$ CFU/g for storage at 0, 4, and 10°C. The lowest population densities were found on days 15, 5, and 3.5 with surviving *V. parahaemolyticus* cells at concentrations of 4.035, 4.019, and 4.069 $\log_{10}$ CFU/g for storage at 0, 4, and 10°C, respectively. The population densities reached the highest values on days 21, 6, and 4.5, respectively, with surviving *V. parahaemolyticus* concentrations of 4.663, 4.893, and 5.138 $\log_{10}$ CFU/g, for 0, 4, and 10°C storage (Fig. 4.3). For the strain containing the *trh* gene, no amplification was detected through real-time PCR.

3. Secondary models of *V. parahaemolyticus* in oysters

Secondary models were developed to describe the parameter changes of primary models as a function of temperature. The IRs obtained from primary TMs and MMs were used to produce secondary TMs and MMs. The Arrhenius model (equation 2) was utilized to describe the change of *V. parahaemolyticus* ln (-IRs) from 0 to 10^{o}C (Fig. 4.4). For the secondary TMs, the coefficients A and E_a/R were 9.156×10^{-10} and -5280.115, respectively (equation 3). The Residual root mean square was 0.154. The R^2 value of goodness of fit was 0.818 after Arrhenius function fitting and the B_f and A_f were 1.003 and 1.048.

$$\ln r = \ln 9.156 \times 10^{-10} + 5280.115 / (273.150 + T) \quad (3)$$

For the secondary MMs, the A and E_a/R values were 7.503×10^{-9} and -4543.456 (equation 4). The RMSE was 0.134, and R^2 value of goodness of fit was 0.812 for Arrhenius equation fitting. B_f and A_f were 1.001 and 1.031.

$$\ln r = \ln 7.503 \times 10^{-9} + 4543.456 / (273.150 + T) \quad (4)$$

4. Validation of secondary MMs in oysters

In order to validate the secondary models of *V. parahaemolyticus* in oysters, the secondary TM was compared with the reported secondary predictive model published (Fernandez-Piquer et al., 2011). Fernandez-Piquer et al. described the effects of storage temperatures from 3.6 to 12.6^{o}C on the survival of *V. parahaemolyticus* in inoculated Pacific oysters (*C. gigas*) (Fernandez-Piquer et al., 2011). The secondary MM in oysters was compared with a secondary validation model built with oysters harvested in different months.

As shown in Fig. 4.5a, both the secondary TM and the reported model had the same decreasing trend: as the temperature increases, the IRs increase. The predicted IRs in the secondary TM of *V. parahaemolyticus* in this study were lower than the predicted IRs in a secondary model reported by Fernandez-Piquer at each given temperature (Fernandez-Piquer et al., 2011). The slope of the secondary TM in this study was greater than that of the reported secondary model. Specifically, the IRs of this model increased more quickly in response to temperature increases than that of the reported model. In Fig. 4.5b, the secondary MM and the validation model nearly overlapped each other. No significant difference was seen between the IRs of the two models ($p = 0.519 > 0.05$). This indicates that the secondary MM in this study is a reliable predictor for IR changes as a result of temperature change.

5. Impact of cold adaptation of *V. parahaemolyticus* on IQF treatment

Oysters inoculated with the *V. parahaemolyticus* cocktail were stored at cold temperatures (0, 4, and 10^{o}C) for 5 days and then treated with IQF treatment. The number of surviving *V. parahaemolyticus* was calculated by both the plate counting method and real-time RT-PCR (*tlh* gene). Based on the plate counting method results, the number of surviving *V. parahaemolyticus* after treatment was below the enumeration limit of the plate counting method (1.95 $\log_{10}$ CFU/g). However, the real-time RT-PCR method found more than 3.888 $\log_{10}$ CFU/g of *V. parahaemolyticus* survived after IQF treatment. As shown in Fig. 4.6, the number of *V. parahaemolyticus* decreased after being stored at 4 and 10 °C for 5 days (comparison between the black bar and the white bar under “before IQF” for storage temperatures at 4 and 10 °C). After the IQF treatment, significant increases in the number of *V. parahaemolyticus* in previously 0, 4, or 10 °C stored oysters were seen (comparison between black bars before and

after treatment in each figure), while significant decreases in the number of *V. parahaemolyticus* in non-low temperature stored oysters were seen (comparison between white bars before and after treatment in each figure) ($P < 0.05$). The increases were 0.553, 0.269, and 0.410 $\log_{10}$ CFU/g, respectively for cold storage temperature of 0, 4, and 10 °C, while the decreases in non-low temperature storage were -0.183, -0.542, and -0.315 $\log_{10}$ CFU/g, respectively.

Discussion

The current study developed RNA-based predictive models to describe the survival of a *V. parahaemolyticus* cocktail in Eastern oysters (*C. virginica*) at cold storage temperatures (0, 4, and 10^{o}C). The predictive MMs showed great potential to predict *V. parahaemolyticus* activities in oysters during post-harvest cold storage. During the past decade, predictive models have been established to describe growth and inactivation of *V. parahaemolyticus* in different broth and seafood matrices (Miles et al., 1997; Yang et al., 2009; Boonyawantang et al., 2012; Parveen et al., 2013). In a recent report, the population of *V. parahaemolyticus* in a Korean oyster slurry decreased when stored at 10 and 15^{o}C for 80 h and 70 h, respectively, with approximate IRs of -0.900 and -1.371 $\log_{10}$ CFU/day. The authors found that the *V. parahaemolyticus* numbers increased in nutrition broth when they were stored at 10 and 15^{o}C (Yoon et al., 2008). Both findings indicated that both the storage temperature and storage conditions such as nutrient concentrations impacted the survival of *V. parahaemolyticus*. It has also been found that the minimum temperature for *V. parahaemolyticus* to grow in tryptic soy broth (TSB) was 5^{o}C (Burnham et al., 2009).

Traditionally, conventional plate counting methods are used to collect data to construct predictive models (Lee et al., 2014; Tang et al., 2015). For instance, TCBS agar is widely used to

enumerate *V. parahaemolyticus* colonies. However, these methods cannot count cells in VBNC or stressed state (Willenburg and Divol, 2012). Almost all of the reported models for *V. parahaemolyticus* in oysters at cold temperature storage did not consider *V. parahaemolyticus* in VBNC or stressed state, which would underestimate the bacterial levels (Fernandez-Piquer et al., 2011; Parveen et al., 2013). In addition, background bacteria may negatively impact the enumeration efficiency of the plating media (Ye et al., 2012). Compared with traditional plate counting methods, molecular quantitative methods can quantify all viable bacteria including cells in VBNC or stressed state (Mishra et al., 2012; Dinu and Bach, 2013). In this study, *V. parahaemolyticus* RNA was extracted and the real-time RT-PCR method was used to construct predictive MMs. RNA is only extracted from live cells which may give more accurate results when using real-time PCR (Derveaux et al., 2010).

In the current study, three storage temperatures (0, 4, and 10^{o}C) were tested. According to Fernandez-Piquer et al, *V. parahaemolyticus* was inactivated when the storage temperature of the oysters was below 12.6^{o}C (Fernandez-Piquer et al., 2011). It is known that *V. parahaemolyticus* stored at low temperatures may enter into the viable but nonculturable (VBNC) or stressed state (Chen et al., 2009) and this has been used to explain why *V. parahaemolyticus* infections continue to happen during summer months (Parveen et al., 2008) even though oyster storage temperatures were usually kept below 10^{o}C. Therefore, to better predict the survival or persistence of *V. parahaemolyticus*, the Baranyi model is utilized to fit the collected data for establishing primary TMs and MMs for *V. parahaemolyticus* in oysters during cold temperature storage in this study (0, 4, and 10^{o}C). The average R^2 of primary TMs was 0.925 and that of primary MMs was 0.859, indicating that the Baranyi model is appropriate to fit data for primary models in this study. The Baranyi model has been used to model the survival of high hydrostatic

pressure treated *Listeria innocua* cells (Saucedo-Reyes et al., 2009) and *Enterobacter sakazakii* in infant formula milk (Pérez et al., 2007) in previous studies. To construct the secondary models, the Arrhenius model was used as it is a common mathematical model to fit bacterial IR data. Fernandez-Piquer et al. applied Arrhenius function to fit a secondary model of *V. parahaemolyticus* in oysters with an R^2 value of 0.78 (Fernandez-Piquer et al., 2011). In our study, the R^2 obtained from TM and MM were greater than 0.8, and B_f and A_f were also within the satisfactory limit ($1.0 < B_f < A_f < 1.1$), which indicated that the two secondary models have a high goodness of fit (Kramer, 2005).

According to the TMs, *V. parahaemolyticus* populations decreased from IVs to FVs with reduction of 2.109, 1.579, and 0.894 $\log_{10}$ CFU/g based on the plate counting results (Fig. 4.2). However, *V. parahaemolyticus* populations reduced by 0.493, 0.362, and 0.238 $\log_{10}$ CFU/g in MMs with no significant difference ($P > 0.05$). As real-time RT-PCR may more sensitively and accurately quantify all of the viable cells (Derveaux et al., 2010), MMs may provide a more accurate and reliable prediction than TMs.

A five-strain *V. parahaemolyticus* cocktail was used in this study, including three non-pathogenic strains with the *tlh* gene, one pathogenic strain with the *tdh* gene and one pathogenic strain with the *trh* gene. *V. parahaemolyticus* infections are mainly caused by *tdh* and *trh* genes (Matsuda et al., 2010; Shimohata and Takahashi, 2010; Yanagihara et al., 2010). In reality, more complicated *V. parhaemolyticus* strain mixtures and micro-flora exist. Thus, models established by using cocktails made with both non-pathogenic and pathogenic strains mimic real contamination situations. The kinetic variations of the pathogenic *V. parahaemolyticus* in the cocktail in oysters were monitored separately by real-time RT-PCR. The population of pathogenic *V. parahaemolyticus* with the *tdh* gene did not significantly decrease

while the population of pathogenic *V. parahaemolyticus* with *trh* gene was not amplified after day 0. A report by Burnham et al. showed that pathogenic *V. parahaemolyticus* (*tdh* positive) decreased by 2.880 and 1.490 $\log_{10}$ CFU/ml in TSB broth when being stored at 5^{o}C and 8^{o}C for 10 days when plating samples on tryptic soy agar (TSA) (Burnham et al., 2009). Another paper reported that pathogenic *V. parahaemolyticus* (*tdh* positive) in salmon had reductions of 3.50, 2.50, and 1.00 $\log_{10}$ CFU/g when stored at 0^{o}C, 3^{o}C, and 9^{o}C respectively for 10 days (plate counting results) (Yang et al., 2009). Although our data is different from previously reported data, two reasons may explain the differences seen. First of all, the methods used were different. This study used real-time RT-PCR to monitor the pathogenic strains in a cocktail used while the previous study used the plate counting method. Secondly, the previous study was done using a single strain not a cocktail. The interaction between pathogenic strains and non-pathogenic strains used in this study may have impacted the final results. Regardless of these differences, all results showed that pathogenic *V. parahaemolyticus* can survive for long periods of time at low temperature storage, which indicates that the pathogenic risk might not be effectively minimized during cold temperature storage.

In order to validate predictive models, the secondary TM was evaluated by comparing it to a reported secondary model of *V. parahaemolyticus* in Pacific oysters (Fernandez-Piquer et al., 2011). In Fig. 4.5, the TM curve was significantly higher than the reported model. The IRs in TM were significantly smaller than those of the reported model at every given temperature ($P < 0.05$). Differences between the two studies may be due to the different oyster species, bacterial strains used, bacterial strain variability, and/or the oyster host defenses. For MM, oysters harvested in summer months were used to validate the model. The MM and validation model were not significantly different ($P > 0.05$).

Individual quick freezing (IQF) (Songsaeng et al., 2010; Muth et al., 2013) is an effective post-harvest processing (PHP) technology. It is applied to treat half-shelled oysters. The National Shellfish Sanitation Program (NSSP) requires that a process needs to reduce *V. parahaemolyticus* in shellfish to an end point of less than 30 CFU/g with a minimum 3.52 Log CFU reduction (FDA, 2013). In this study, inoculated oysters with or without 5-day cold storage were treated by IQF. The surviving *V. parahaemolyticus* was monitored by both the traditional plate counting method and the real-time RT-PCR method. The plate counting method did not generate any numbers after incubation as the number of the surviving *V. parahaemolyticus* was below the limit of enumeration (1.95 Log CFU/g). However, the real-time PCR results showed that the surviving population of *V. parahaemolyticus* in cold-adapted samples was significantly higher compared to the non-cold adapted samples after IQF treatment. The cold storage enhanced the capability of *V. parahaemolyticus* to resist IQF treatment. Similar results have been reported by others. Lin et al. reported that survival of *V. parahaemolyticus* subjected to cold shock treatment increased after being stored at 5 or -18^{o}C for a period of 4 to 6 days (Lin et al., 2004). Chen et al. showed that *V. parahaemolyticus* changed morphologies from rod-shape to coccoid under cold stress, which might facilitate bacterial stress adaptation (Chen et al., 2009). In addition, in a pathogenic *V. parahaemolyticus* prevalence study, the authors found that pathogenic *V. parahaemolyticus* could be isolated from iced and frozen seafood products, which indicates that low temperature could hardly be considered to eliminate the public health hazard in contaminated seafood (Yang et al., 2008).

In summary, this study developed and validated RNA-based molecular predictive models to describe the survival of *V. parahaemolyticus* in oysters during cold temperature storage (0, 4, and 10^{o}C). Compared with traditional models (TMs) which were built based on plate counting

methods, molecular models (MMs) give a more accurate evaluation of the surviving cells as it counts all viable *V. parahaemolyticus* cells. Among the *V. parahaemolyticus* strains studied, pathogenic *V. parahaemolyticus* with the *tdh* gene showed no significant reduction ($P > 0.05$). By comparing the cold adapted and the non-cold adapted *V. parahaemolyticus* treated with IQF, the results indicated that the cold adapted *V. parahaemolyticus* had increased resistance to cold processing. Cold-adaptation generated a negative impact on the efficiency of IQF treatment and reveal that it is important to have a more reliable and accurate predictive model system to better assist with *V. parahaemolyticus* risk assessment and management in seafood.

References

Arrhenius S. 1915. Quantitative laws in biological chemistry. G. Bell and Sons, Ltd., London, United Kingdom.

Baranyi J, Roberts TA, McClure P. 1993. A non-autonomous differential equation to model bacterial growth. Food Microbiol. **10:** 43-59.

Boonyawantang A, Mahakarnchanakul W, Rachtanapun C, Boonsupthip W. 2012. Behavior of pathogenic *Vibrio parahaemolyticus* in prawn in response to temperature in laboratory and factory. Food Control **26:** 479-485.

Burnham VE, Janes ME, Jakus LA, Supan J, DePaola A, Bell J. 2009. Growth and survival differences of *Vibrio vulnificus* and *Vibrio parahaemolyticus* strains during cold storage. J. Food Sci. **74:** 314-318.

Chen SY, Jane WN, Chen YS, Wong HC. 2009. Morphological changes of *Vibrio parahaemolyticus* under cold and starvation stresses. Int. J. Food Microbiol. **129:** 157-165.

Cheney DP. 2010. Bivalve shellfish quality in the USA: from the hatchery to the consumer. J. World Aquac. Soc. **41:** 192-206.

DaSilva L, Parveen S, DePaola A, Bowers J, Brohawn K, Tamplin ML. 2012. Development and validation of a predictive model for the growth of *Vibrio vulnificus* in postharvest shellstock oysters. Appl. Environ. Microbiol. **78:** 1675-1681.

Derveaux S, Vandesompele J, Hellemans J. 2010. How to do successful gene expression analysis using real-time PCR. Methods **50:** 227-230.

Dinu LD, Bach S. 2013. Detection of viable but non-culturable *Escherichia coli* O157: H7 from vegetable samples using quantitative PCR with propidium monoazide and immunological assays. Food Control **31:** 268-273.

Elexson N, Son R, Rukayadi Y, Zainazor TT, Ainy MN, Nakaguchi Y, Mitsuaki N. 2013. Biosafety of *Vibrio Parahaemolyticus* biofilm from seafood using herbs and spices. J. Life Med. **1:** 71-82.

Fernandez-Piquer J, Bowman JP, Ross T, Tamplin ML. 2011. Predictive models for the effect of storage temperature on *Vibrio parahaemolyticus* viability and counts of total viable bacteria in Pacific oysters (*Crassostrea gigas*). Appl. Environ. Microbiol. **77:** 8687-8695.

Food and Drug Administration (FDA), Interstate Shellfish Sanitation Conference (ISSC). 2013, National Shellfish Sanitation Program (NSSP): Guide for the Control of Molluscan Shellfish. 2013 Revision. Washington, DC.

Garnier M, Labreuche Y, Garcia C, Robert M, Nicolas JL. 2007. Evidence for the involvement of pathogenic bacteria in summer mortalities of the Pacific oyster *Crassostrea gigas*. Microb. Ecol. **53:** 187-196.

Hunt DA, Miescier J, Redman J, Salinger A, Lucas JP. 1984. Molluscan shellfish, fresh or fresh frozen oysters, mussels or clams. Compendium of methods for the microbiological examination of foods. 590-610.

Iwamoto M, Ayers T, Mahon BE, Swerdlow DL. 2010. Epidemiology of seafood-associated infections in the United States. Clin. Microbiol. Rev. **23:** 399-411.

Kramer M. 2005. R2 statistics for mixed models. In Proceedings of the conference on applied statistics in agriculture (Vol. 17, pp. 148-160).

Lee YJ, Jung BS, Yoon HJ, Kim KT, Paik HD, Lee JY. 2014. Predictive model for the growth kinetics of *Listeria monocytogenes* in raw pork meat as a function of temperature. Food Control **44:** 16-21.

Liao C, Peng ZY, Li JB, Cui XW, Zhang ZH, Malakar PK, Zhang WJ, Pan YJ, Zhao Y. 2015. Simultaneous construction of PCR-DGGE-based predictive models of *Listeria monocytogenes* and *Vibrio parahaemolyticus* on cooked shrimps. Lett. Appl. Microbiol. **60:** 210-216.

Lin C, Yu RC, Chou CC. 2004. Susceptibility of *Vibrio parahaemolyticus* to various environmental stresses after cold shock treatment. Int. J. Food Microbiol. **92:** 207-215.

Matsuda S, Kodama T, Okada N, Okayama K, Honda T, Iida T. 2010. Association of *Vibrio parahaemolyticus* thermostable direct hemolysin with lipid rafts is essential for cytotoxicity but not hemolytic activity. Infect. Immun. **78:** 603-610.

Meujo DA, Kevin DA, Peng J, Bowling JJ, Liu J, Hamann MT. 2010. Reducing oyster-associated bacteria levels using supercritical fluid CO^2 as an agent of warm pasteurization. Int. J. Food Microbiol. **138:** 63-70.

Miles DW, Ross T, Olley J, McMeekin TA. 1997. Development and evaluation of a predictive model for the effect of temperature and water activity on the growth rate of *Vibrio parahaemolyticus*. Int. J. Food Microbiol. **38:** 133-142.

Mishra A, Taneja N, Sharma M. 2012. Viability kinetics, induction, resuscitation and quantitative real-time polymerase chain reaction analyses of viable but nonculturable *Vibrio cholerae* O1 in freshwater microcosm. J. Appl. Microbiol. **112:** 945-953.

Muth MK, Viator CL, Karns SA, Cajka JC, O'Neil M. 2013. Analysis of the costs and economic feasibility of requiring postharvest processing for raw oysters. Compr. Rev. Food Sci. Food Saf. **12:** 652-661.

Parveen S, Hettiarachchi KA, Bowers JC, Jones JL, Tamplin ML, McKay R, Beatty W, Brohawn K, DaSilva LV, DePaola A. 2008. Seasonal distribution of total and pathogenic

Vibrio parahaemolyticus in Chesapeake Bay oysters and waters. Int. J. Food Microbiol. **128:** 354-361.

Parveen S, DaSilva L, DePaola A, Bowers J, White C, Munasinghe KA, Brohawn K, Mudoh M, Tamplin, M. 2013. Development and validation of a predictive model for the growth of *Vibrio parahaemolyticus* in post-harvest shellstock oysters. Int. J. Food Microbiol. **161:** 1-6.

Pérez P, Aliaga RD, Reyes SD, López MA. 2007. Pressure inactivation kinetics of *Enterobacter sakazakii* in infant formula milk. J. Food Prot. **70:** 2281-2289.

Postollec F, Falentin H, Pavan S, Combrisson J, Sohier D. 2011. Recent advances in quantitative PCR (qPCR) applications in food microbiology. Food Microbiol. **28:** 848-861.

Ramamurthy T, Ghosh A, Pazhani GP, Shinoda S. 2014. Current perspectives on viable but non-culturable (VBNC) pathogenic bacteria. Front. Public Health **2:** 103.

Rudi K, Moen B, Dromtorp SM, Holck AL. 2005. Use of ethidium monoazide and PCR in combination for quantification of viable and dead cells in complex samples. Appl. Environ. Microbiol. **71:** 1018-1024.

Saucedo-Reyes D, Marco-Celdrán A, Pina-Pérez MC, Rodrigo D, Martínez-López A. 2009. Modeling survival of high hydrostatic pressure treated stationary-and exponential-phase *Listeria innocua* cells. Innov. Food Sci. Emerg. Technol. **10:** 135-141.

Shimohata T, Takahashi A. 2010. Diarrhea induced by infection of *Vibrio parahaemolyticus*. J. Med. Invest. **57:** 179-182.

Sobrinho PDSC, Destro MT, Franco BD, Landgraf M. 2014. A quantitative risk assessment model for *Vibrio parahaemolyticus* in raw oysters in Sao Paulo State, Brazil. Int. J. Food Microbiol. **180:** 69-77.

Songsaeng S, Sophanodora P, Kaewsrithong J, Ohshima T. 2010. Quality changes in oyster (*Crassostrea belcheri*) during frozen storage as affected by freezing and antioxidant. Food Chem. **123:** 286-290.

Su CP, Jane WN, Wong HC. 2013. Changes of ultrastructure and stress tolerance of *Vibrio parahaemolyticus* upon entering viable but non-culturable state. Int. J. Food Microbiol. **160:** 360-366.

Su YC, Liu C. 2007. *Vibrio parahaemolyticus*: a concern of seafood safety. Food Microbiol. **24:** 549-558.

Tang X, Zhao Y, Sun X, Xie J, Pan Y, Malakar PK. 2015. Predictive model of *Vibrio parahaemolyticus* O3: K6 growth on cooked *Litopenaeus vannamei*. Ann. Microbiol. **65:** 487-493.

Tse TPY. 2015. Virulence gene expression of *Vibrio parahaemolyticus* in the viable but nonculturable state (Doctoral dissertation, California Polytechnic State University, San Luis Obispo).

Wagner AO, Malin C, Knapp BA, Illmer P. 2008. Removal of free extracellular DNA from environmental samples by ethidium monoazide and propidium monoazide. Appl. Environ. Microbiol. **74:** 2537-2539.

Willenburg E, Divol B. 2012. Quantitative PCR: an appropriate tool to detect viable but not culturable *Brettanomyces bruxellensis* in wine. Int. J. Food Microbiol. **160:** 131-136.

Yanagihara I, Nakahira K, Yamane T, Kaieda S, Mayanagi K, Hamada D, Fukui T, Ohnishi K, Kajiyama S, Shimizu T, Sato M, Ikegami T, Ikeguchi M, Honda T, Hashimoto H. 2010. Structure and functional characterization of *Vibrio parahaemolyticus* thermostable direct hemolysin. J. Biol. Chem. **285:** 16267-16274.

Yang ZQ, Jiao XA, Zhou XH, Cao GX, Fang WM, Gu RX. 2008. Isolation and molecular characterization of *Vibrio parahaemolyticus* from fresh, low-temperature preserved, dried, and salted seafood products in two coastal areas of eastern China. Int. J. Food Microbiol. **125:** 279-285.

Yang ZQ, Jiao XA, Li P, Pan ZM, Huang JL, Gu RX, Fang WM, Chao GX. 2009. Predictive model of *Vibrio parahaemolyticus* growth and survival on salmon meat as a function of temperature. Food Microbiol. **26:** 606-614.

Ye K, Wang H, Zhang X, Jiang Y, Xu X, Zhou G. 2013. Development and validation of a molecular predictive model to describe the growth of *Listeria monocytogenes* in vacuum-packaged chilled pork. Food Control **32:** 246-254.

Ye M, Huang Y, Chen H. 2012. Inactivation of *Vibrio parahaemolyticus* and *Vibrio vulnificus* in oysters by high-hydrostatic pressure and mild heat. Food Microbiol. **32:** 179-184.

Yoon KS, Min KJ, Jung YJ, Kwon KY, Lee JK, Oh SW. 2008. A model of the effect of temperature on the growth of pathogenic and nonpathogenic *Vibrio parahaemolyticus* isolated from oysters in Korea. Food Microbiol. **25:** 635-641.

Zhang ZH, Liu HQ, Lou Y, Xiao LL, Liao C, Malakar PK, Pan YJ, Zhao Y. 2015. Quantifying viable *Vibrio parahaemolyticus* and *Listeria monocytogenes* simultaneously in raw shrimp. Appl. Microbiol. Biotechnol. **99:** 6451-6462.

Table 4.1. *Vibrio parahaemolyticus* strains used in this study

Strains	**Strain number**	**Virulence gene**	**Isolation**
V. parahaemolyticus	ATCC 17802	*trh* / *tlh*	Shirasu food poisoning, Japan
V. parahaemolyticus	ATCC 43996	*tdh* / *tlh*	Cockles causing fatal food poisoning, England
V. parahaemolyticus	ATCC 27969	*tlh*	Crustacean, USA
V. parahaemolyticus	*V. p.* 12	*tlh*	Oysters, USA
V. parahaemolyticus	*V. p.* 21	*tlh*	Oysters, USA

Table 4.2. Inactivation parameters of primary molecular and traditional models

		Molecular model	**Traditional model**
0°C	R^2	0.881	0.943
	Initial value (log_{10} CFU/g)	5.428 ± 0.0477	5.601 ± 0.167
	Final value (log_{10} CFU/g)	4.935 ± 0.0177	3.492 ± 0.0955
	Lag time (day)	0	1.931 ± 0.528
	Inactivation rate (log_{10} CFU/d)	-0.134 ± 0.0263	-0.245 ± 0.05
4°C	R^2	0.891	0.931
	Initial value (log_{10} CFU/g)	5.114 ± 0.0335	5.293 ± 0.138
	Final value (log_{10} CFU/g)	4.752 ± 0.0125	3.714 ± 0.0718
	Lag time (day)	0	1.605 ± 0.559
	Inactivation rate (log_{10} CFU/d)	-0.0886 ± 0.0184	-0.152 ± 0.0434
10°C	R^2	0.806	0.902
	Initial value (log_{10} CFU/g)	5.261 ± 0.0345	5.463 ± 0.0467
	Final value (log_{10} CFU/g)	5.023 ± 0.0205	4.569 ± 0.0783
	Lag time (day)	0	0
	Inactivation rate (log_{10} CFU/d)	-0.073 ± 0.0168	-0.121 ± 0.0635

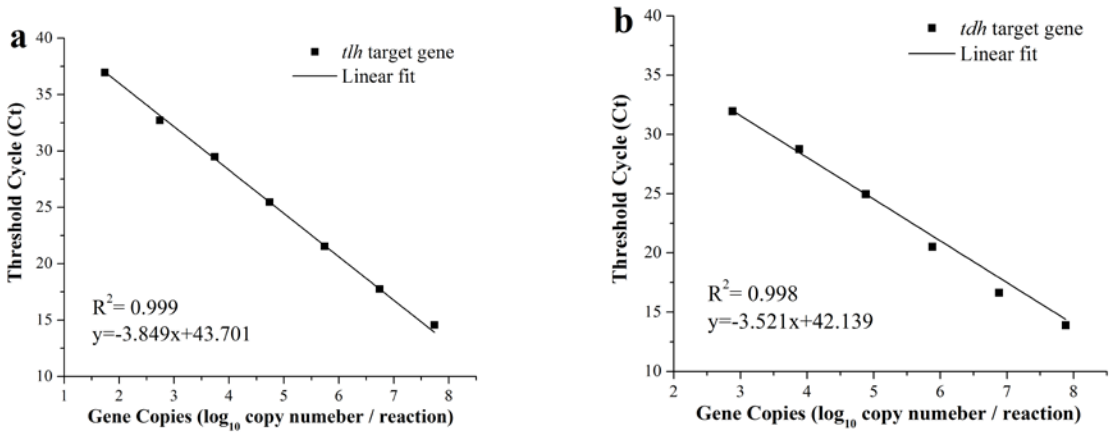

Figure 4.1. Standard curves used for *V. parahaemolyticus tlh* and *tdh* gene quantification by real-time RT-PCR

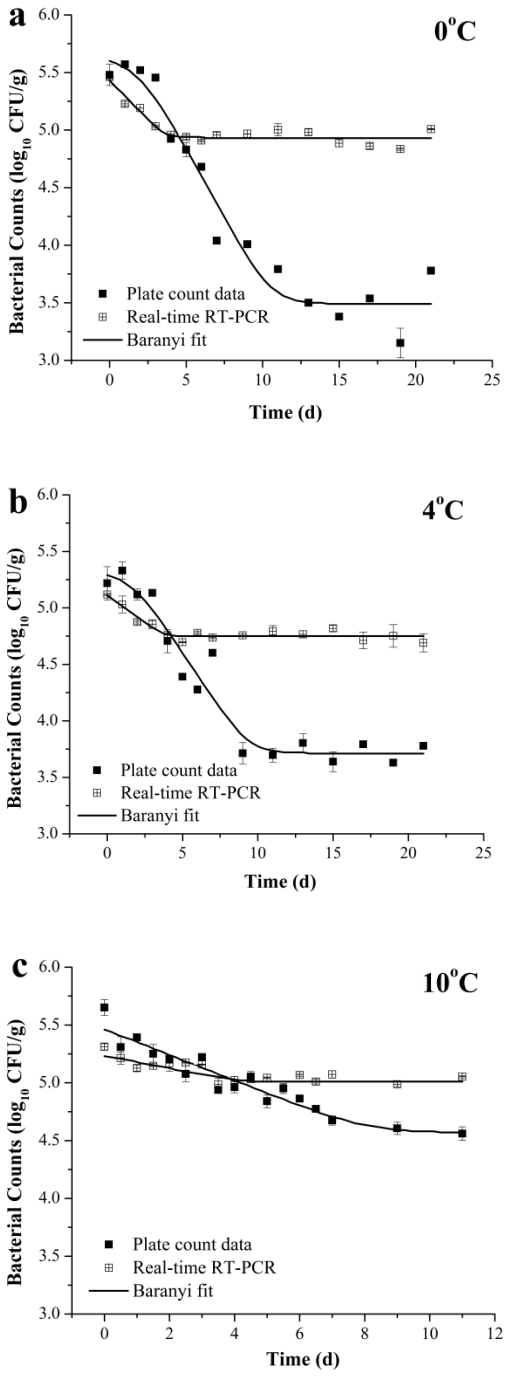

Figure 4. 2. Primary molecular models (MMs) established based on *tlh* gene and primary traditional models (TMs) based on the plate counting method of *V. parahaemolyticus* after being stored at 0, 4, and 10°C for 21, 21, and 11 days.

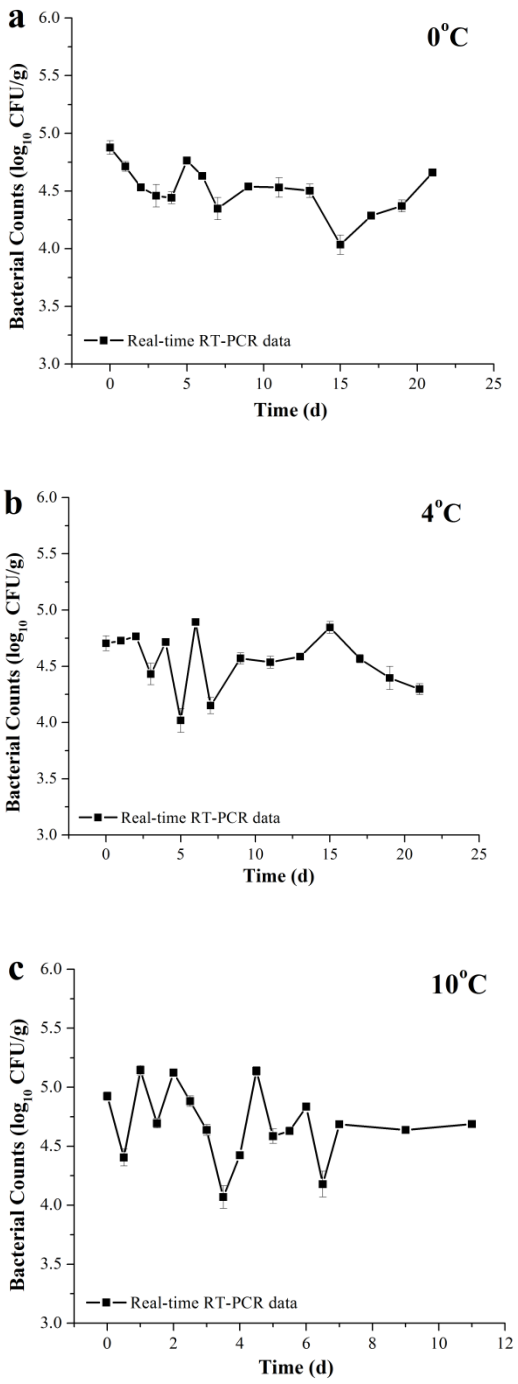

Figure 4.3. Surviving pathogenic *V. parahaemolyticus* (with *tdh* gene) in oysters during cold storage monitored by real-time RT-PCR.

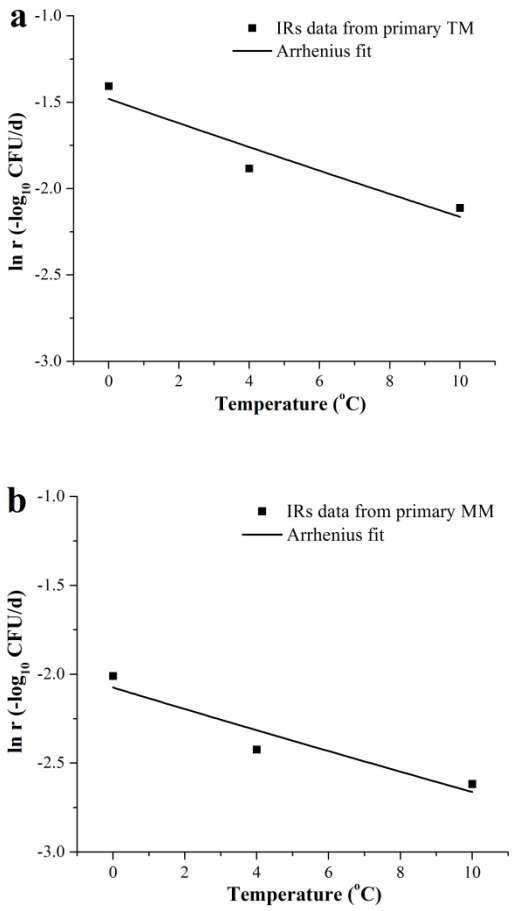

Figure 4.4. (a) Secondary traditional model established based on primary tradition models (TMs); (b) Secondary molecular model established based on primary molecular model (MMs).

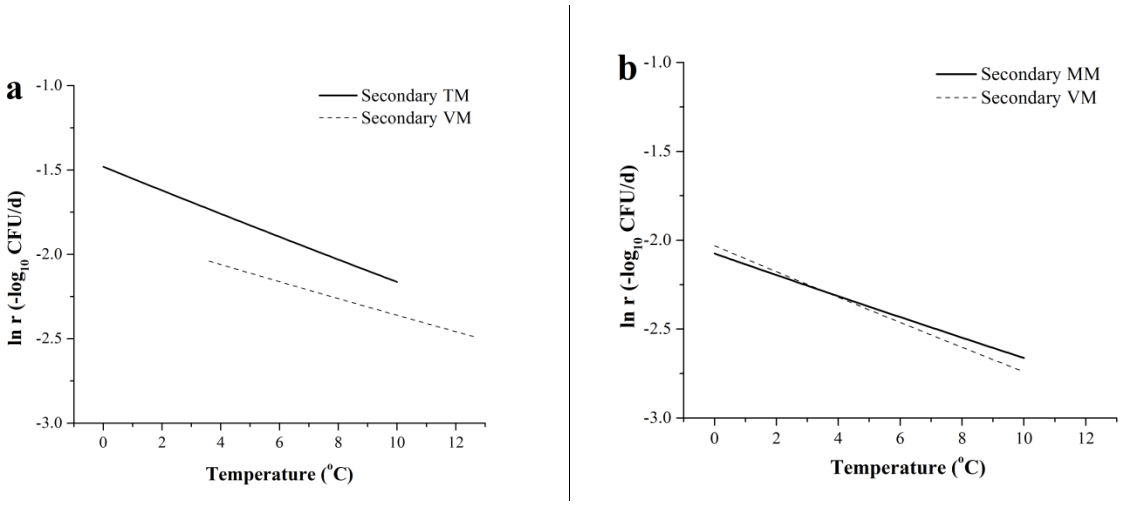

Figure 4.5. Validation of secondary models (a) Comparison of secondary traditional model (Secondary TM) in this study and the inactivation model reported by Fernandez-Piquer et al. (2011) (Secondary VM); (b) Comparison of secondary molecular model (Secondary MM) in this study and validation model (Secondary VM) also established in this study.

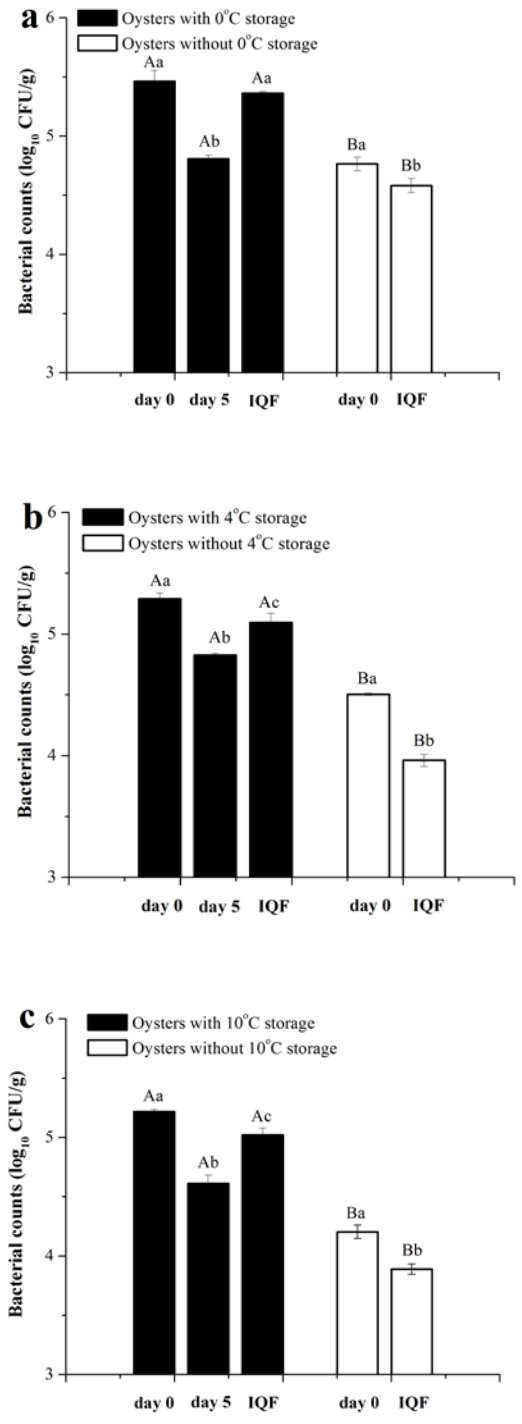

Figure 4.6. Number of surviving *V. parahaemolyticus* cells in cold and non-cold stored oysters after IQF treatment. (a) Number of surviving *V. parahaemolyticus* in oysters with 0oC storage for 5 days and then IQF treatment (black bars), inoculated oysters without 0oC storage but direct

IQF (white bars); (b) Number of surviving *V. parahaemolyticus* in oysters with 4oC storage for 5 days and then IQF treatment (black bars), inoculated oysters without 4oC storage but direct IQF (white bars); (c) Number of surviving *V. parahaemolyticus* in oysters with 10oC storage for 5 days and then IQF treatment (black bars), inoculated oysters without 10oC storage but direct IQF (white bars). Different uppercase letters on the bars indicate significant differences ($P < 0.05$) present between the number of *V. parahaemolyticus* in the oysters with cold storage and without cold storage. Different lowercase letters on the bars indicate significant differences ($P < 0.05$) present between the number of *V. parahaemolyticus* in oysters before and after IQF treatment. The concentration of *V. parahaemolyticus* in oysters without cold storage (0, 4, and 10oC) at Day 0 is approximate to that in oysters with cold storage (0, 4, and 10oC) at Day 5.

Chapter 5: Summary

In recent years, *Vibrio parahemolyticus* has become the leading cause of foodborne illnesses in seafood, which makes its consumption a potential risk to human health. Quantitative microbial risk assessment (QMRA) has been applied as a strong tool to evaluate and control pathogenic bacteria so as to improve food safety. As an important part, predictive models provide data of pathogen growth or survival in seafood to support QMRA. Currently, a number of studies on predictive models of *V. parahaemolyticus* in seafood under different conditions have been undertaken. Almost all the predictive models are constructed based on traditional plate counting methods, traditional models (TMs). However, plate counting methods have been found to be time-consuming, labor-intensive, and cannot enumerate the bacteria in the viable but non-culturable (VBNC) or stressed state induced at cold temperature. The TMs based on plate counting methods might underestimate the population of *V. parahaemolyticus* in seafood at cold temperature storage.

In this thesis, molecular models (MMs) using DNA-based PCR-DGGE and RNA-based real-time RT-PCR were constructed to estimate the survival and susceptibility of *V. parahaemolyticus* in seafood (cooked shrimps and postharvest oysters) stored at cold temperature (0, 4, 10^{o}C). We found MMs can be more accurate and sensitive than TMs to predict the amount of *V. parahaemolyticus*, because the VBNC and stressed cells can be quantified through the extracted DNA or RNA. However, DNA can be extracted from dead cells without being fully lysed, leading to overrating quantitative results due to some *V. parahaemolyticus* dying at low temperatures. Therefore, MMs based on real-time RT-PCR provide the most accurate prediction of *V. parahaemolyticus* in seafood when stored at low temperature (0, 4, and

10^{o}C). The RNA-based MMs can be the promising tool to provide reliable data to support QMRA for improving food safety.